

# Applications of Raman spectroscopy to the study of graphitic carbons in the Earth sciences

The Raman spectrum of graphitic carbons: Theory

Characterizing graphitic carbons by Raman spectroscopy: Methodology



Olivier Beyssac & Michele Lazzari  
CNRS IMPMC Paris  
(olivier.beyssac or michele.lazzari @impmc.upmc.fr)

## 1. Introduction

### **2. The Raman spectrum of graphitic carbons: Theory**

- 2.1. Why are the D and 2D peaks so 'unique'?
- 2.2. Basic concepts of quantum mechanics and perturbation theory
- 2.3. Electronic gap and resonant Raman
- 2.4. Fourth-order perturbation and double resonant Raman
- 2.5. Electronic structure and phonon dispersion in graphene/graphite
- 2.6. Double resonance in graphite
- 2.7. Attribution of the Raman peaks
- 2.8. Shape and width of the 2D peak
- 2.9. Intensity of the D peak and the Tuinstra-Koenig relation

### **3. Methodology: characterizing graphitic carbons by Raman microscopy**

- 3.1. Raman spectroscopy is a surface analysis of graphitic carbons
- 3.2. Analytical strategy and sample preparation: how to minimize analytical artifact?
- 3.3. The anisotropic structure of graphitic carbons and polarization effects
- 3.4. Dispersion of the defect peaks and choice of a laser wavelength
- 3.5. Fitting spectra: how to retrieve quantitative information on the structure of graphitic carbons
- 3.6. The intrinsic structural heterogeneity of natural graphitic carbons

### **4. Applications of Raman spectroscopy to the study of natural graphitic carbons**

- 4.1. Carbonization/graphitization during terrestrial diagenesis/metamorphism
- 4.2. Graphitic carbons and fluid-rock interactions
- 4.3. Graphitic carbons as traces of life in the geological record
- 4.4. Graphitic carbons and cosmochemistry
- 4.5. Graphitic carbons and environmental Sciences

## 5. Conclusion

**Graphitic carbons** are

**amorphous-like or turbostratic or microcrystalline or  
Monocrystalline...**

**opaque** (high extinction coefficient for visible light)

=> Low penetration of laser, <200 nm (Lespade et al. 1984)

**anisotropic** (increasing anisotropy with graphitization)

=> Possible effect of sample orientation vs laser polarization

**fragile** (easily cleaved along the graphene layers)

**heterogeneous** (in terms of structure and chemistry)



# Chemical and structural evolution of carbonaceous material during burial

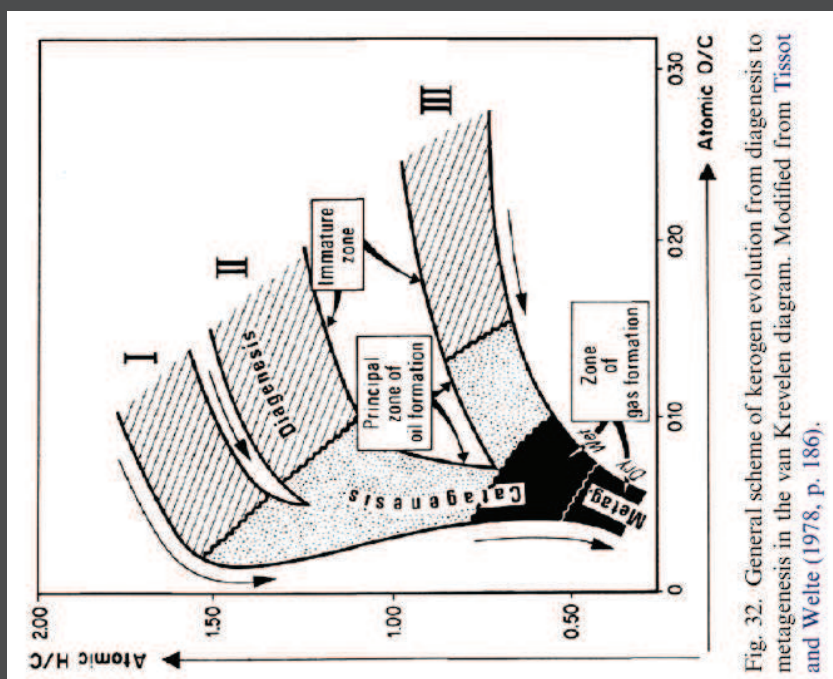
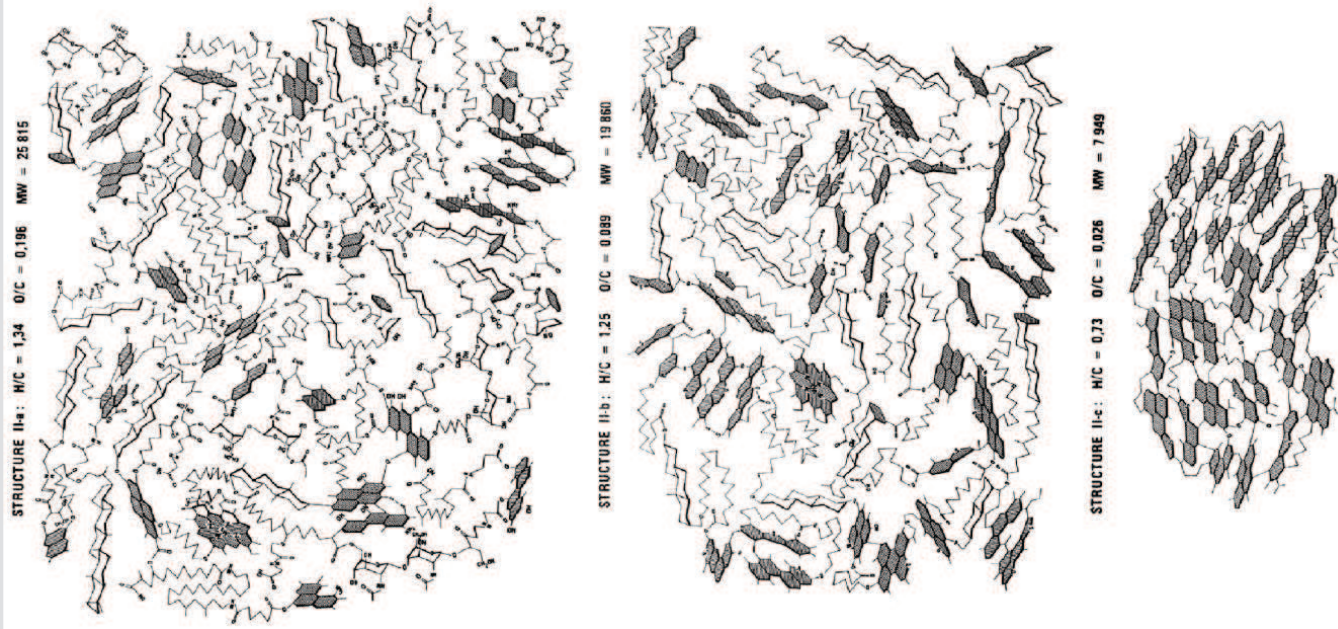


Fig. 32. General scheme of kerogen evolution from diagenesis to metagenesis in the van Krevelen diagram. Modified from Tissot and Welte (1978, p. 186).



Review by  
Vandenbroucke & Largeau,  
*Organic Geochemistry* (2007)

Fig. 57. Structural representation of Type II kerogen (analytical data from Paris Basin Toarcian series) at increasing maturity stages, corresponding to given atomic H/C and O/C ratios. Structure IIa: beginning of diagenesis; structure IIb: beginning of catagenesis; structure IIc: end of catagenesis. Adapted from Behar and Vandenbroucke (1987).

# Quantifying the degree of graphitization

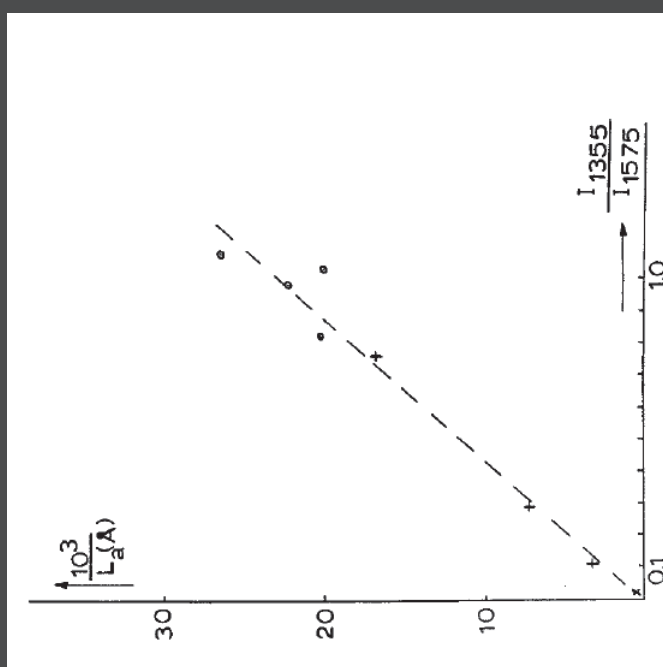
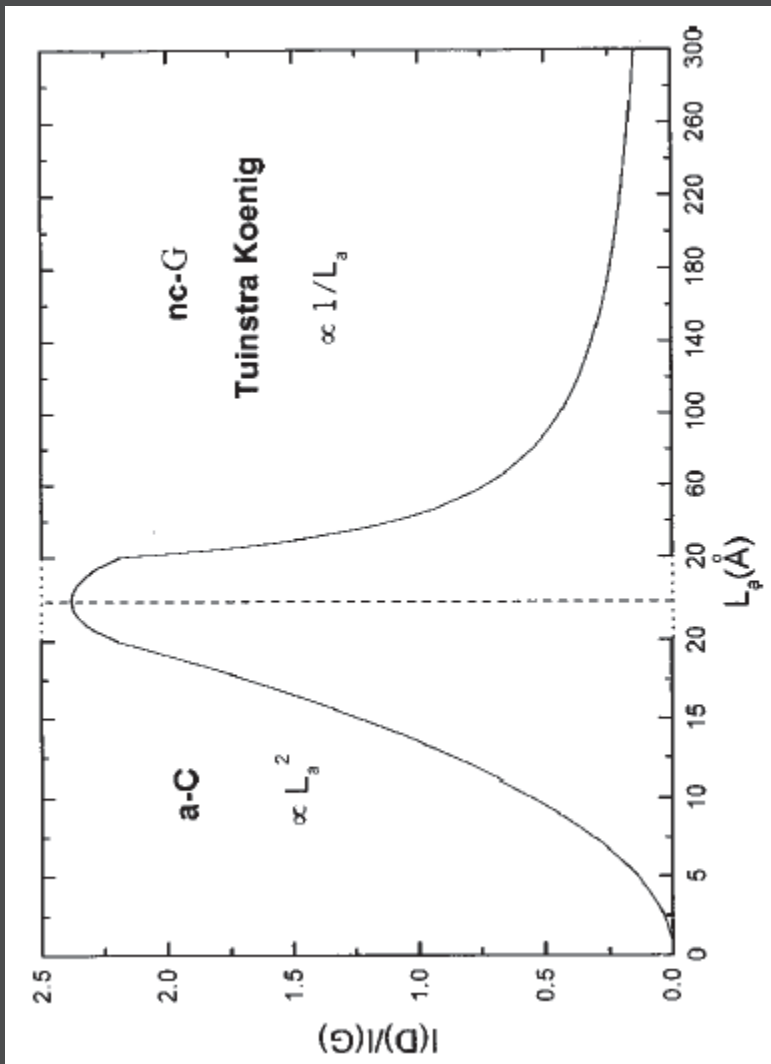


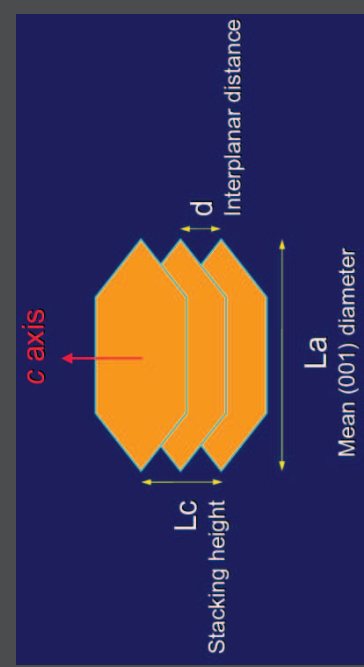
Fig. 3. Calibration of Raman intensities versus x-ray data of  $L_a$ . ○, data and samples furnished by Dr. S. L. Strong (Union Carbide). +, samples prepared following directions in [G. M. Arnold, carbon 5, 33 (1967)]. X, stress annealed pyrolytic graphite.

Tuinstra & Koenig, J. Chem. Phys., 1970



Ferrari and Robertson, Phys. Rev. B, 2000

$$\frac{I(D)}{I(G)} = \frac{C'(\lambda)L_a^2}{L_a},$$



For a review: Beyssac & Lazzeri EMU Notes in Mineralogy 2012

## Protocol for Raman analysis of graphitic carbon materials

Raman spectroscopy is a **surface analysis** for graphitic carbons

Dispersivity of the defect bands => constant laser  $\lambda$  (514.5 nm)

Laser-induced heating => low-laser power (<0.5mW @ 514.5 nm)

Sample orientation versus laser polarization => **not a problem except for graphite monocrystals**

Structural defects induced by sample preparation (e.g. polishing) => **analysis below a transparent mineral** within the thin-section thickness

Intrinsic **structural heterogeneity** of natural graphitic carbons => to be documented

Extracting quantitative information from the Raman spectra => **Peak fitting**

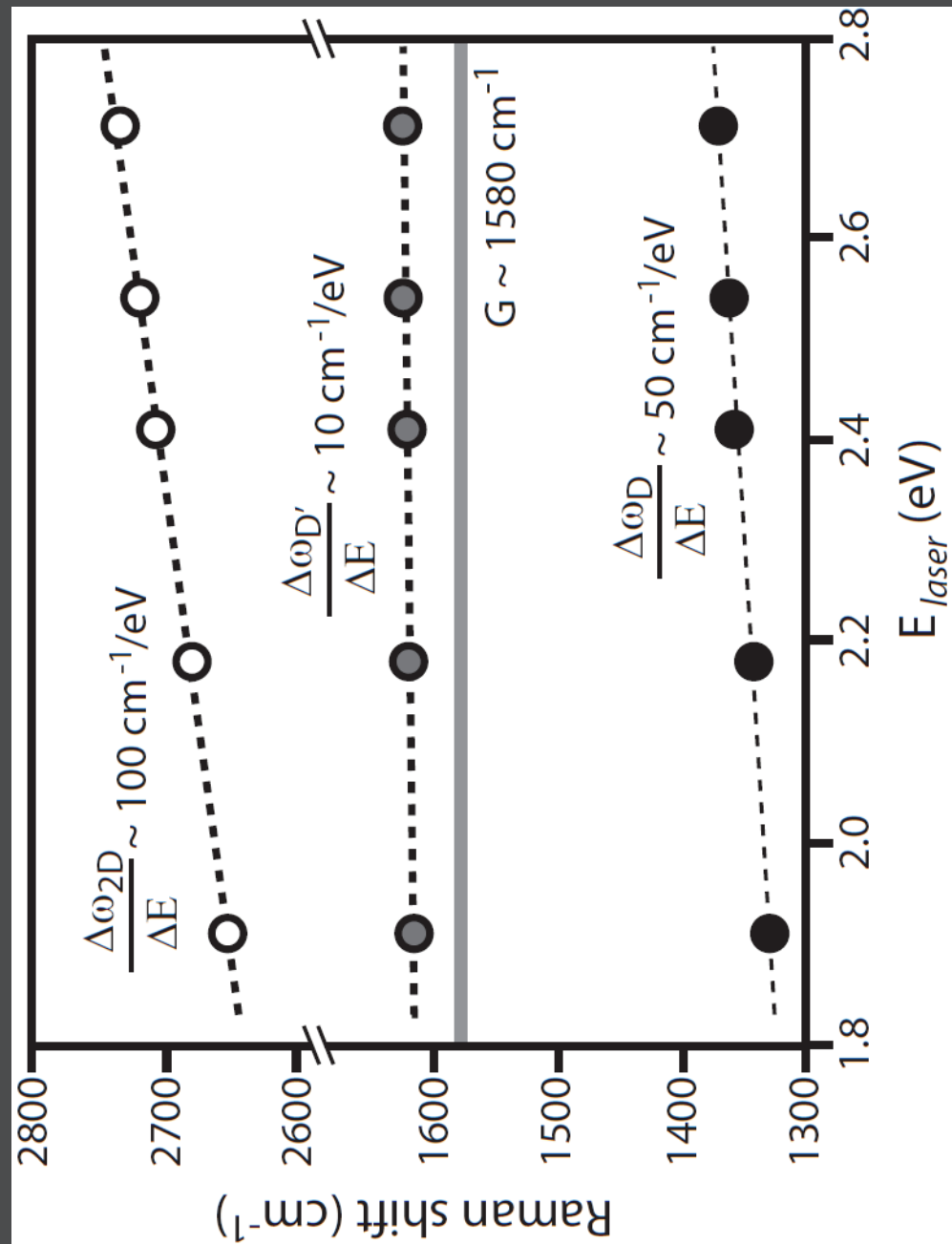
...

See Beyssac & Lazzari, EMU Notes in Mineralogy and references therein

## Dispersivity of the defect bands: practical consequences

---

position and relative intensities=f( $\lambda_{laser}$ )



## Dispersivity of the defect bands: practical consequences

position and relative intensities=f( $\lambda_{\text{laser}}$ )

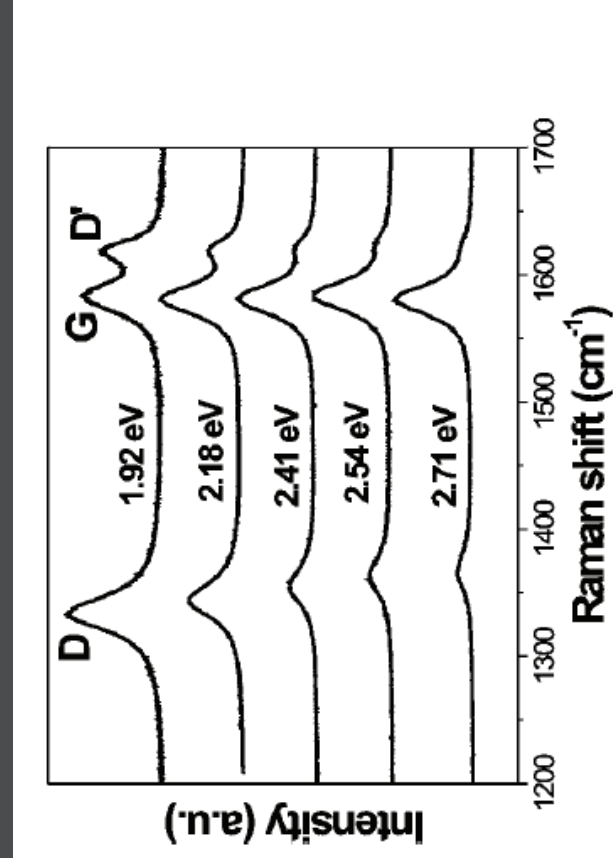


FIG. 2. (Color online) Raman spectra of the sample heat treated at 2000 °C, for five different laser energy values (1.92, 2.18, 2.41, 2.54, and 2.71 eV).

**Spectra to be compared MUST be obtained  
at the very same laser wavelength**

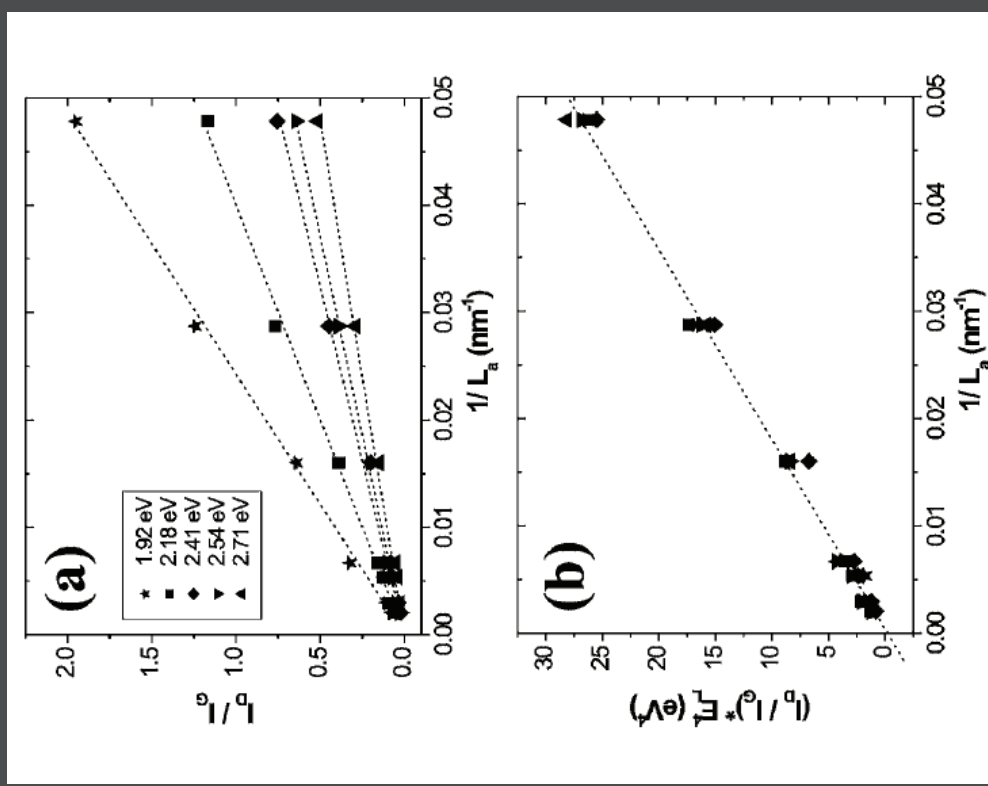
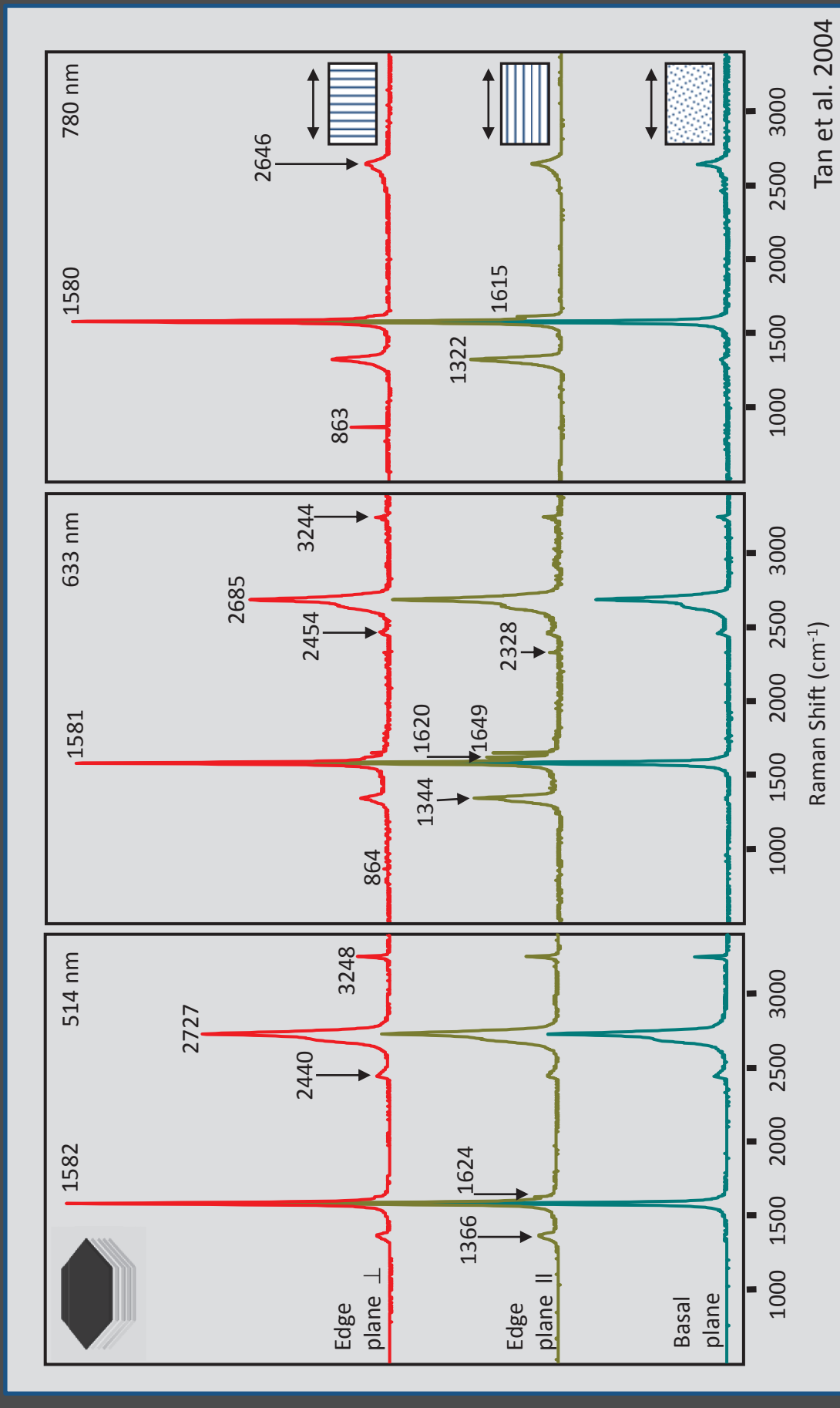


FIG. 3. (Color online) (a) Plot of the ratio of the integrated intensities of the D and G bands ( $I_D/I_G$ ) vs  $1/L_a$  for all spectra obtained with the five different excitation laser energies. (b) All experimental results shown in part (a) collapse in the same straight line in the  $(I_D/I_G)E_l^4$  vs  $1/L_a$  plot.

## Sample orientation versus laser polarization

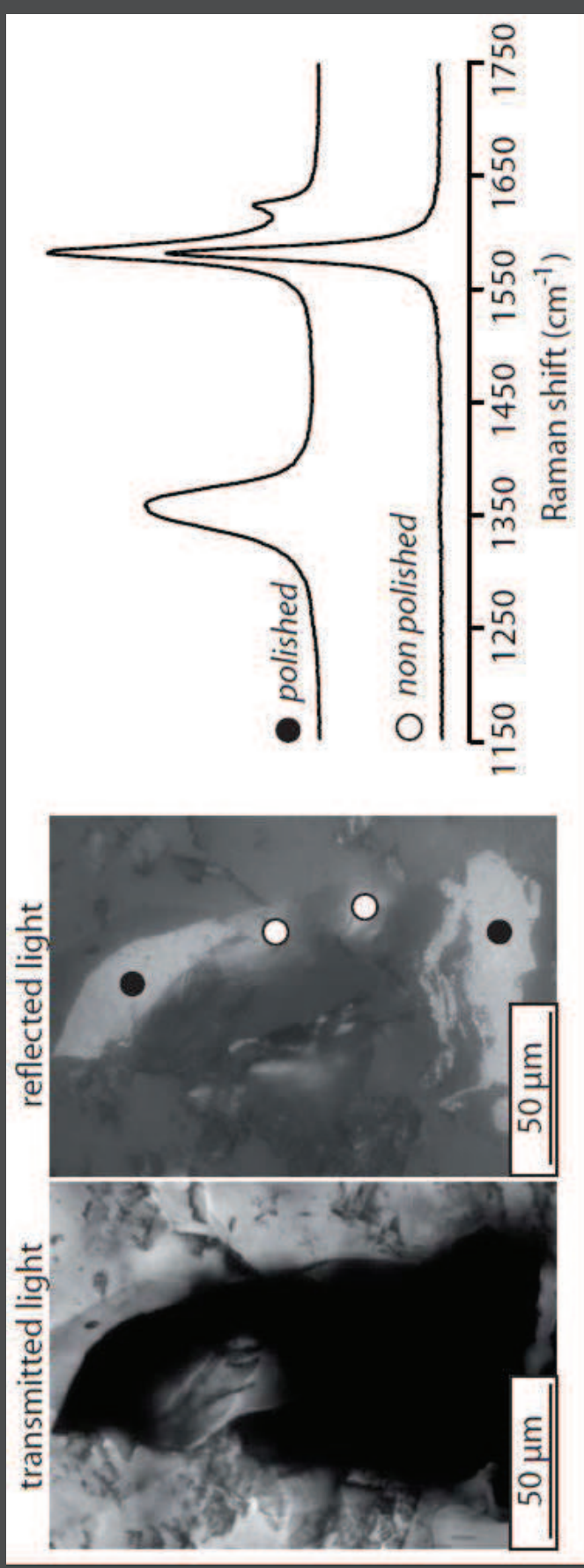


No significant effect @ 514 nm for graphitic C / microcrystalline graphite  
For graphite monocrystal, use a circular polarization for the laser and measure same orientation

## Structural defect induced by sample preparation (polishing, crushing, chemistry...)

---

Graphitic carbons are black, opaque materials, and as such have a high extinction coefficient for visible light. The direct consequence is that, in the visible range, the penetration of the laser in graphitic carbons is very low. Using C films with a well constrained thickness deposited by chemical vapor deposition on a corundum substrate, Lespade *et al.* (1984) estimated the argon laser ( $2.41\text{eV}$ ,  $514\text{ nm}$ ) penetration depth at about  $100\text{-}200\text{ nm}$ .



## Structural defect induced by sample preparation (polishing, crushing, chemistry...)

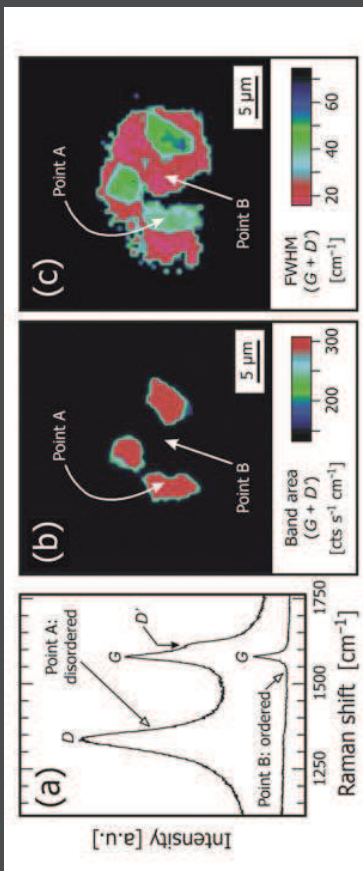
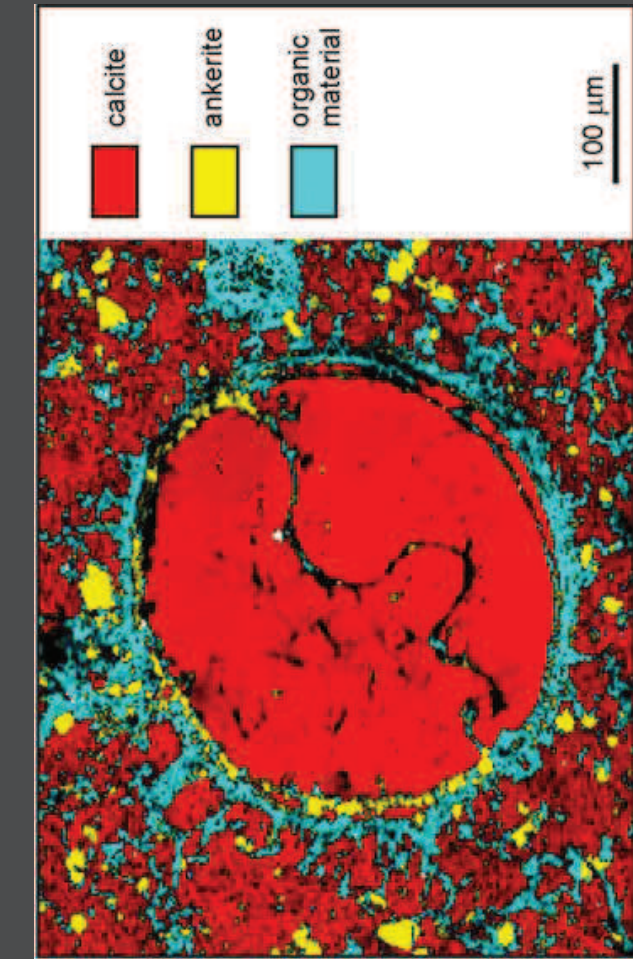


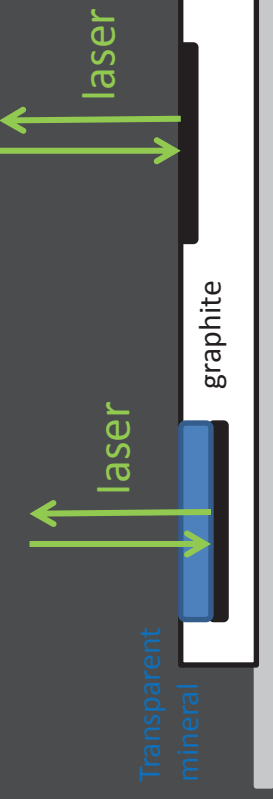
**Fig. 19.** Raman maps of a graphite flake in a metacarbonate (sample no. AL8-1; courtesy of A. Lepland) from the 3.8 Ga Isua Supracrustal Belt, Greenland, showing that graphite disorder can be induced by the polishing process. **(a)** The two Raman spectra show that graphite that has been exposed to the surface of the thin section is disordered (spectrum A) whereas the main graphite flake, analysed through a thin chlorite cover, appears well-ordered (spectrum B). **(b)** A Raman map of the surface, generated from the integral intensity of the band at  $\sim 1600 \text{ cm}^{-1}$ , shows three micro-areas in which graphite is exposed at the surface. This map corresponds widely to an optical microphotograph taken in the reflected light mode (not shown). **(c)** A Raman map, recorded with the focus of the fully focused beam adjusted  $\sim 2 \mu\text{m}$  below the surface and generated from the broadening of the  $\sim 1600 \text{ cm}^{-1}$  band, shows that only the three exposed areas have experienced structural disorder (large FWHMs) as a result of the mechanical polishing process. Surrounding micro-areas that are still covered by chlorite are well ordered (smaller FWHMs).

Nasdala et al. (EMU notes 2004)



Bernard et al. (EPSL 2007)

Non polished  
polished



Analysis below a transparent  
mineral within the thin-section  
thickness  
⇒ No structural mapping on  
polished sample.

## Laser-induced heating

Photo-oxydation of graphitic C  
under the laser in air

Downshifting of G and D position

→ Must use low-laser energy  
( $< 0.5\text{mW}$  @ 514.5 nm)

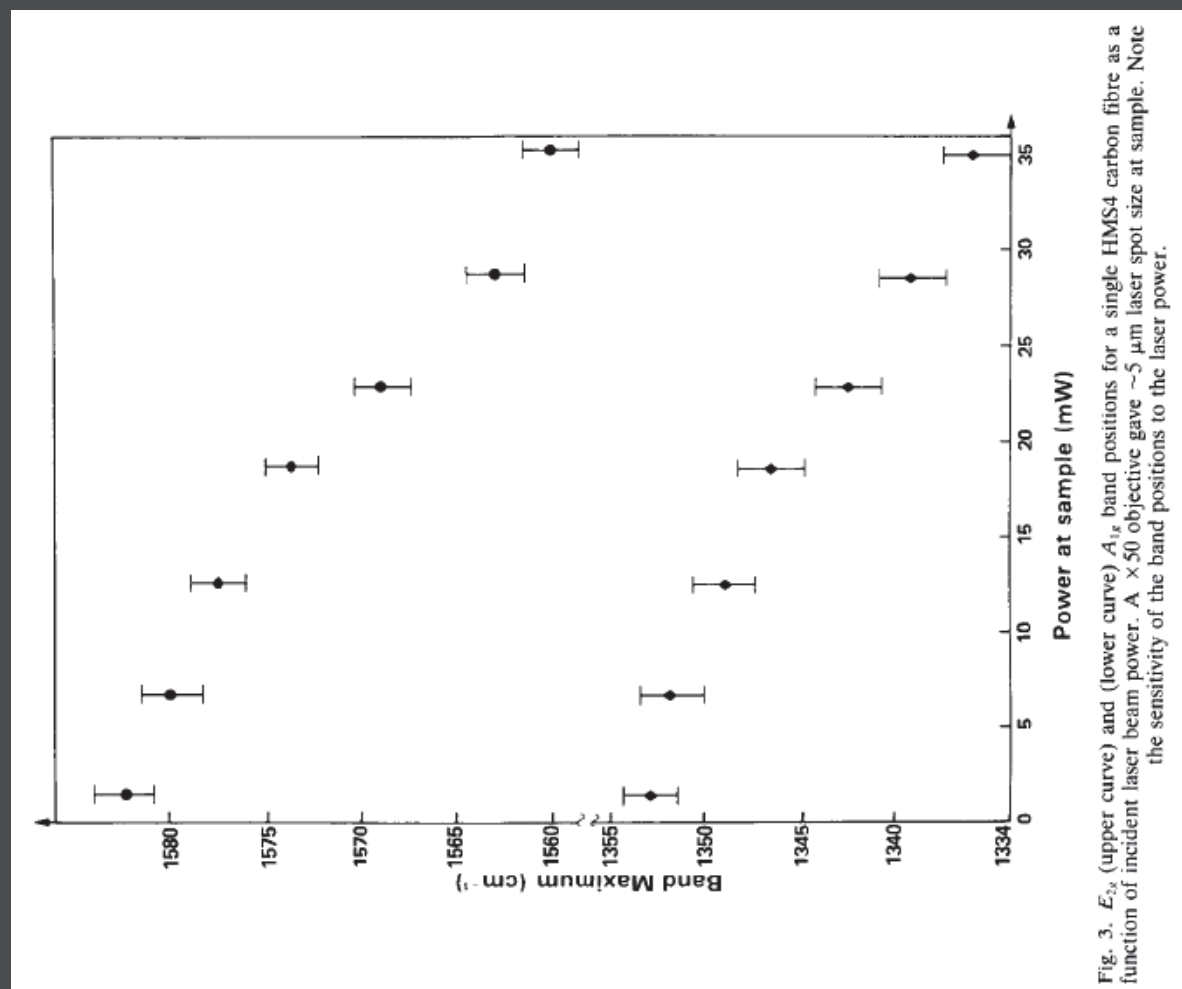
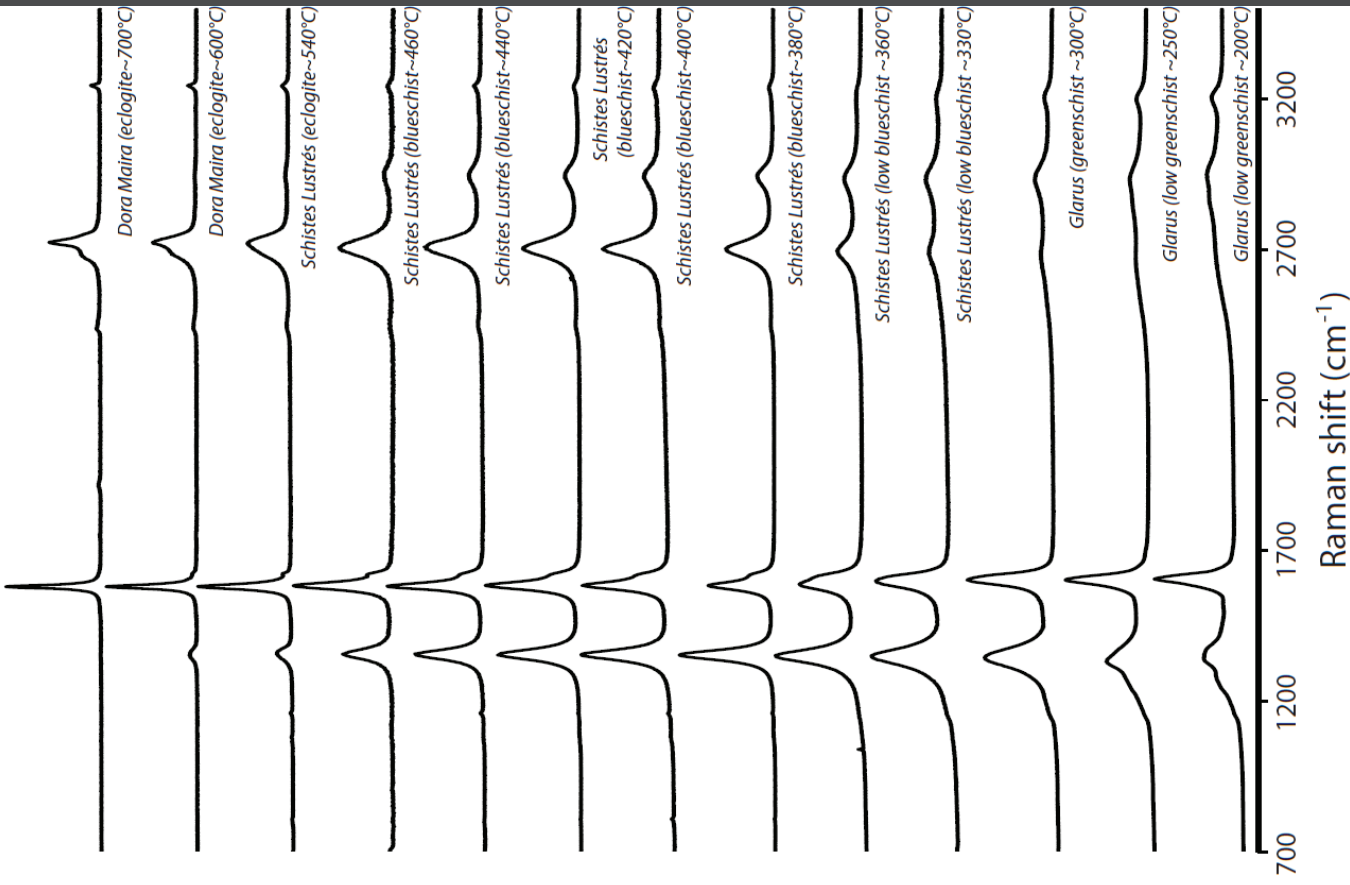


Fig. 3.  $E_{2g}$  (upper curve) and (lower curve)  $A_{1g}$  band positions for a single HMS4 carbon fibre as a function of incident laser beam power. A  $\times 50$  objective gave  $\sim 5 \mu\text{m}$  laser spot size at sample. Note the sensitivity of the band positions to the laser power.

# Raman spectroscopy of graphitic carbons



**Double-resonance Raman theory for the defect Bands (Thomsen & Reich 2000; see Beyssac & Lazzeri EMU notes in Mineralogy for a review)**

Frequency (cm <sup>-1</sup> )	Peak designation	Other peak designation	Raman process <sup>(1)</sup>	Remarks
1100	D''		D1P	Graphene – Martins Ferreira <i>et al.</i> (2010)
1200	D	D1 D3 G	D1P (D2P) IP E <sub>2g</sub>	Soots – Sadezky <i>et al.</i> (2005)
1350	(D''+D <sup>4</sup> )	D <sup>4</sup>	D1P	Natural carbons – Lahfid <i>et al.</i> (2010)
1500	G	D <sup>3</sup>	D1P	Soots, amorphous carbons – Sadezky <i>et al.</i> (2005)
1580	D'		D2P	
1620	D''	D2	D1P	
2450	D+D''		2P	
2700	2D	S1	2P	
2950	D+D'/D+G	S2	D2P	
3240	2D'		2P	
3260	G+D'		D2P	Graphene – Martins Ferreira <i>et al.</i> (2010)

<sup>(1)</sup> Raman process is one-phonon (1P), two-phonons (2P), defect-activated one-phonon (D1P), defect-activated two-phonons (D2P).

**Beyssac & Lazzeri  
EMU Notes 2012**

## Raman versus XRD (tracking 3D ordering)

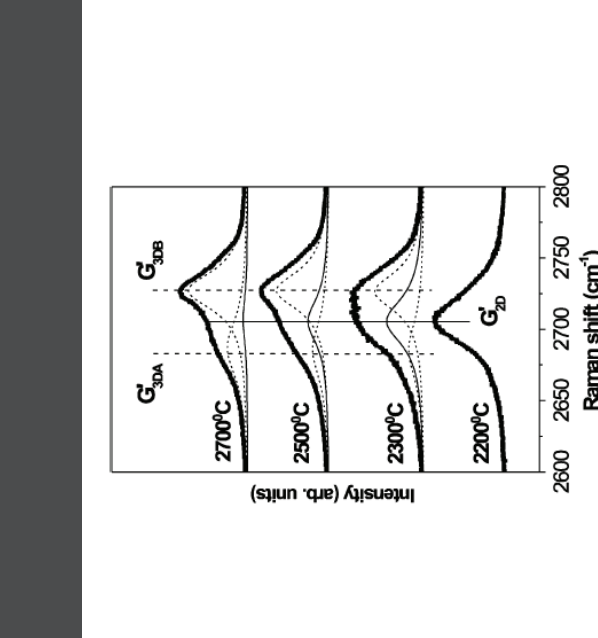


Fig. 16  $G'$  band Raman spectra of samples heat treated to various temperatures  $T_{\text{hut}}$ , performed using  $E_{\text{laser}} = 2.41 \text{ eV}$  (514.5 nm). The  $G'$  band changes from one peak to two peaks with increasing  $T_{\text{hut}}$ .  
Pimenta et al. (2007)

Splitting of the 2D band indicates  
Local 3D ABAB stacking

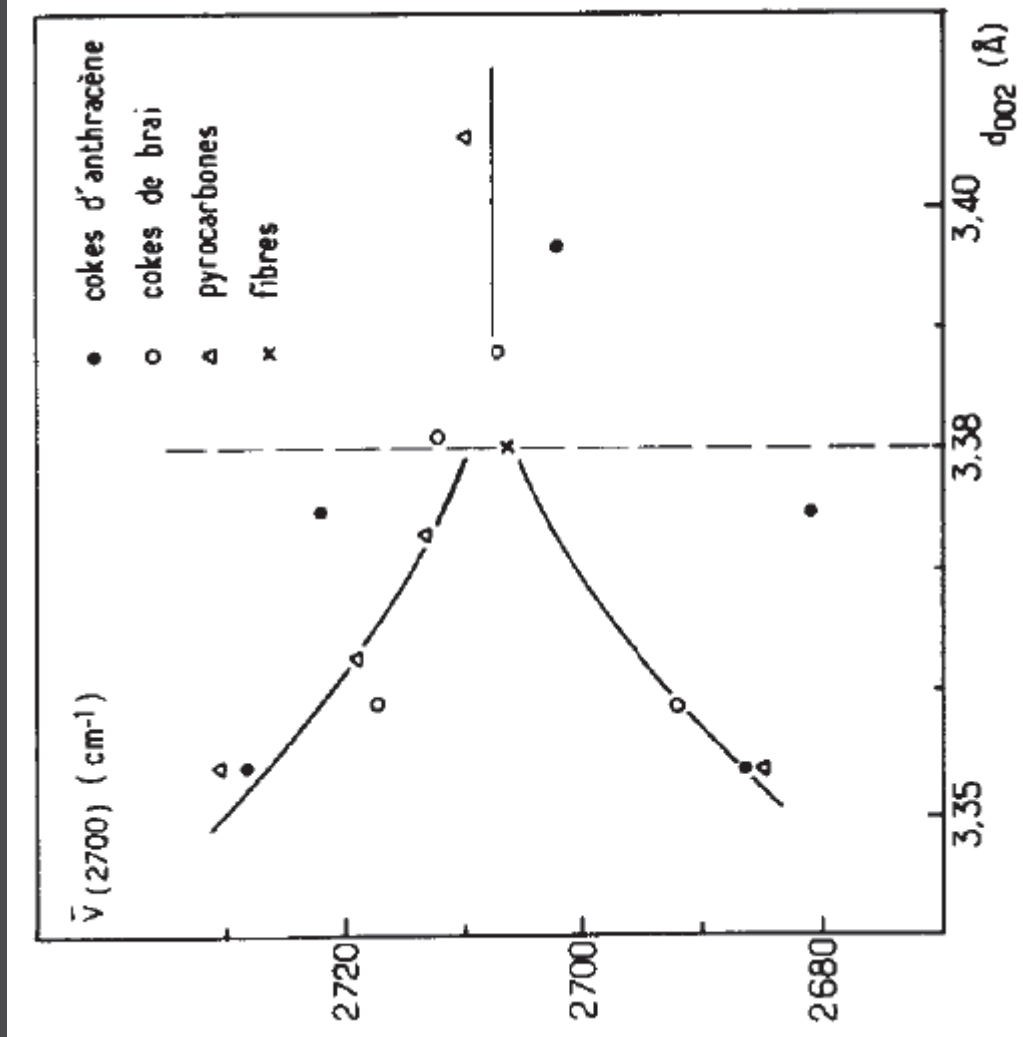
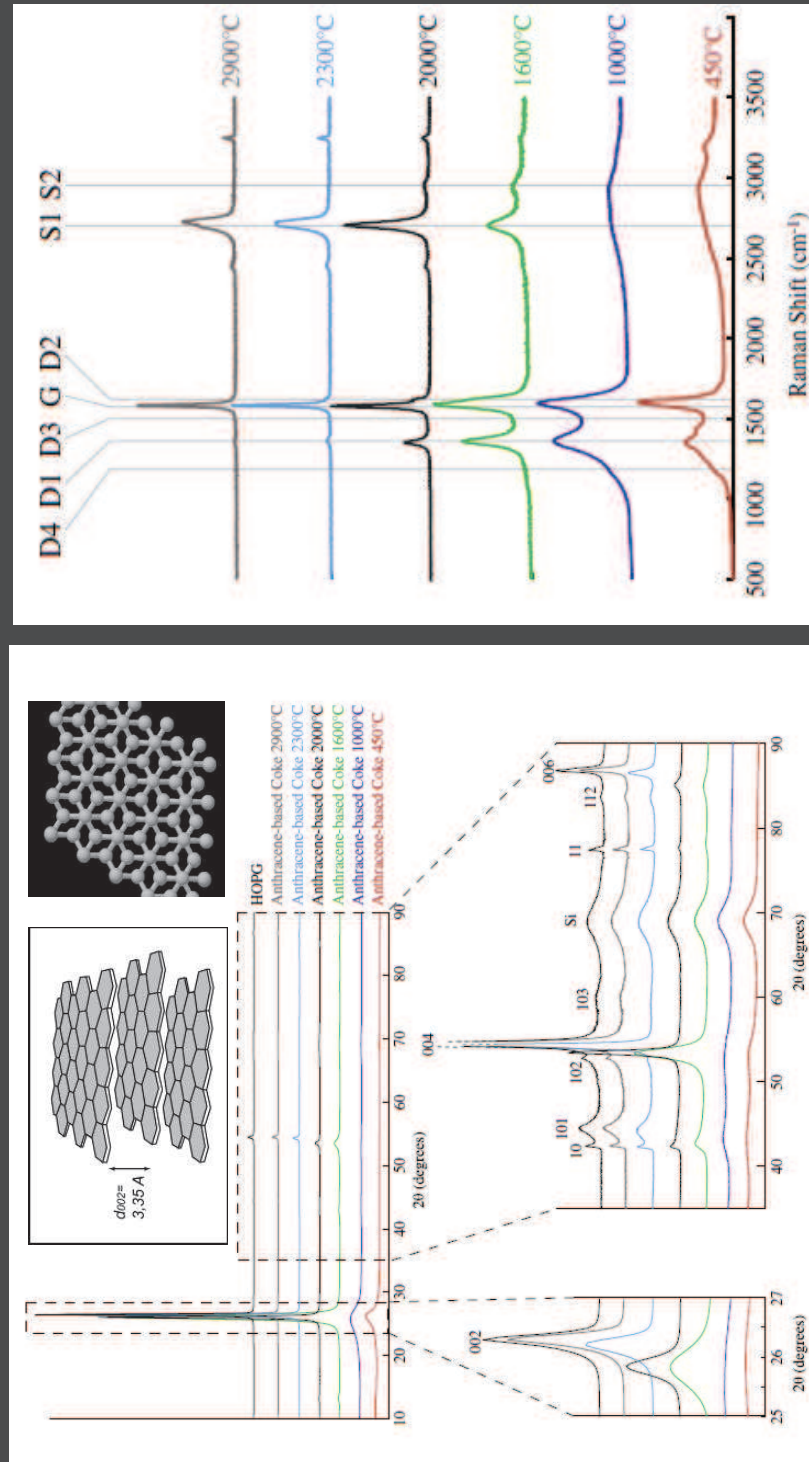


Fig. 7. Dédoublement de la raie située vers  $2700 \text{ cm}^{-1}$ .

Lespade et al. (Carbon 1984)

## Raman versus XRD (tracking 3D ordering)



Bernard et al. (Carbon 2010)

	XRD	HRTEM	Raman
Sample preparation	destructive: bulk separates	destructive: bulk separates	nondestructive: in situ in thin sections or rock powders
Size of sample	bulk technique	hundreds of Ångströms	$\mu\text{m}^3$
Scale	macro	micro	mini
Crystallite dimension measured	$d(L_c, L_a)$	$d(L_c, L_a)$	$L_u(L_c)$
Information about crystallite size	indirect	direct	indirect
Analysis time	slow because of required sample preparation	very slow because of scale and complexity of analysis	relatively fast because of minimal sample preparation and scale of analysis

+ STXM-XANES  
At the C k-edge

Wopenka & Pasteris (Am Min 1993)

## Fitting spectra of graphitic carbons

Bonal et al. (GCA 2006)

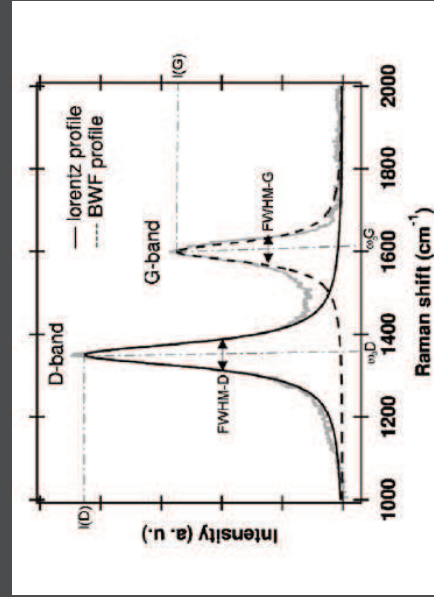


Fig. 1. Raman spectra of a polycyclic aromatic carbonaceous material, intensity in arbitrary unit (a.u.). The D-band was fitted by a Lorentzian profile and the G-band by a Breit-Wigner-Fano profile to obtain the spectral parameters FWHM-D,  $I_0$ ,  $I_G$ ,  $\omega_0D$ ,  $\omega_0G$ .

Sadezky et al., Carbon, 2005

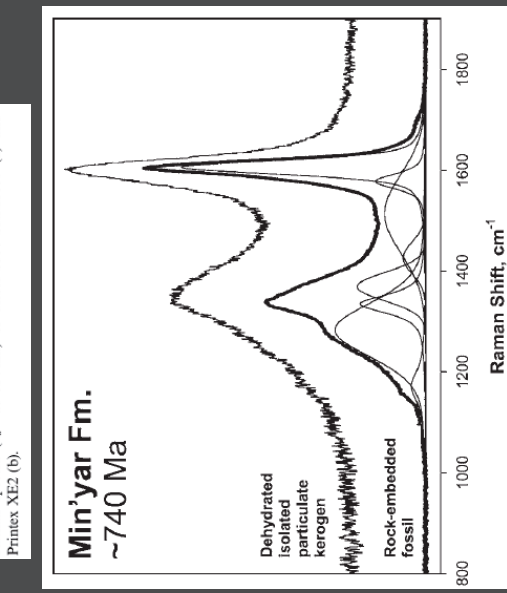
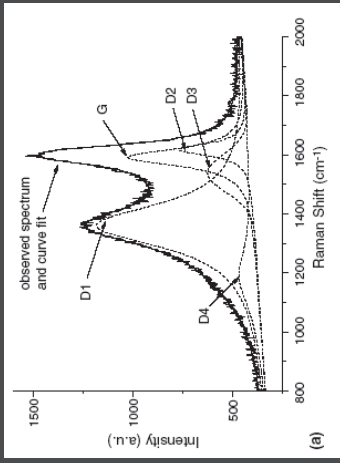


Fig. 7. Curve fit with band combination (IX) for the first-order Raman spectra ( $\lambda_0$  = at 514 nm) of diesel soot SRM1630 (a) and Printex XE2 (b).

Zickler et al. (Carbon 2006)

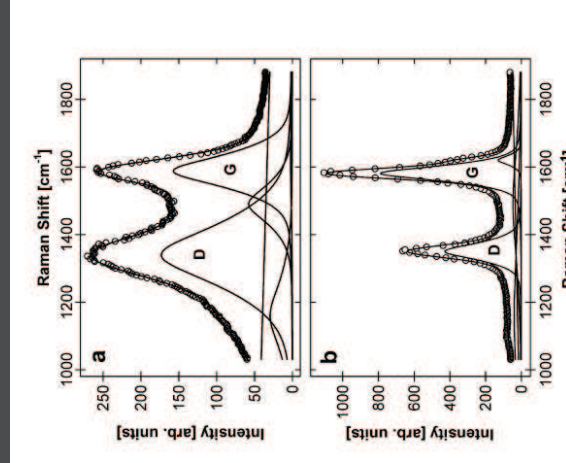
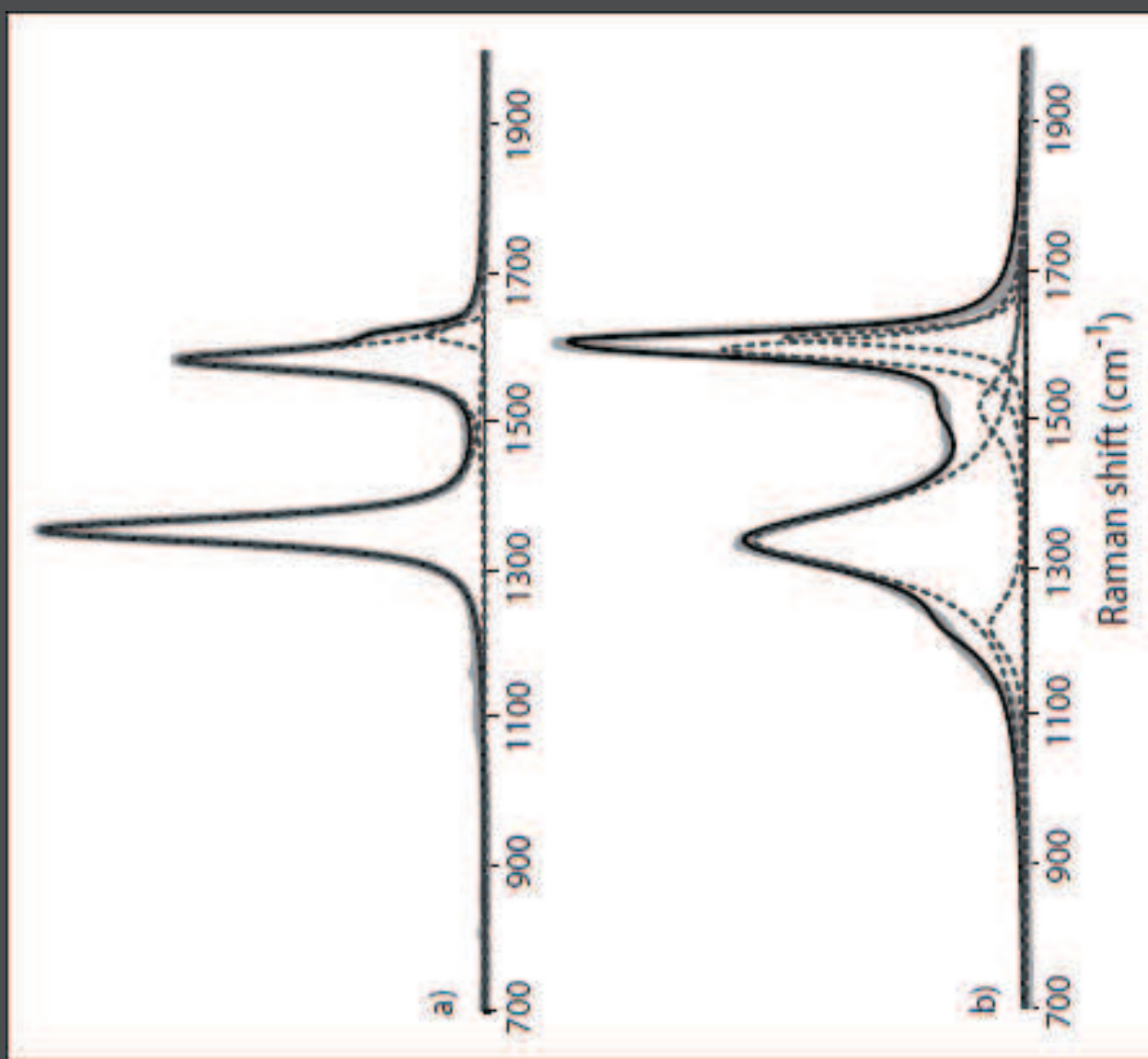


Fig. 5. Raman spectra for spruce wood pyrolyzed at 900 °C (a) and for the carbon fiber HTA-21 (b). The circles indicate the measured intensities and the solid lines represent the fitted Raman curve with the corresponding Raman bands (see text).

Schopf et al. (Astrobiology 2005)

## Fiting spectra of graphitic carbons

Examples of peak-fitting procedures for Raman spectra of graphitic carbons. a) Peak-fitting in case of a very disordered graphitic carbon using 5 bands with pure Lorentzian shape. b) Peak-fitting in case of a graphitic carbon using 3 bands with Voigt profile (mix Gaussian-Lorentzian). Note that in all cases no *a priori restriction* is imposed on the band position, FWHM or intensity. Thick grey line is the measured spectrum, black line is the modeled spectrum, grey dashed lines are the peaks modeled.



Extraction of quantitative parameters (FWHM, position, ratios...)  
Caution with  $I_D / I_G$  ratio

# The Raman spectrum of graphite: theory

Michele Lazzari

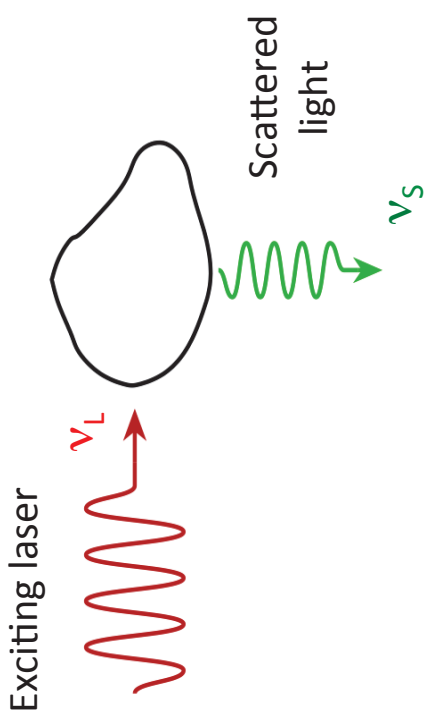
IMPMC, CNRS, UPMC (Univ. Paris 6), France

- Graphite: model for sp<sub>2</sub> carbons
- Present unique features (theoretical understanding not easy)
- Very well studied

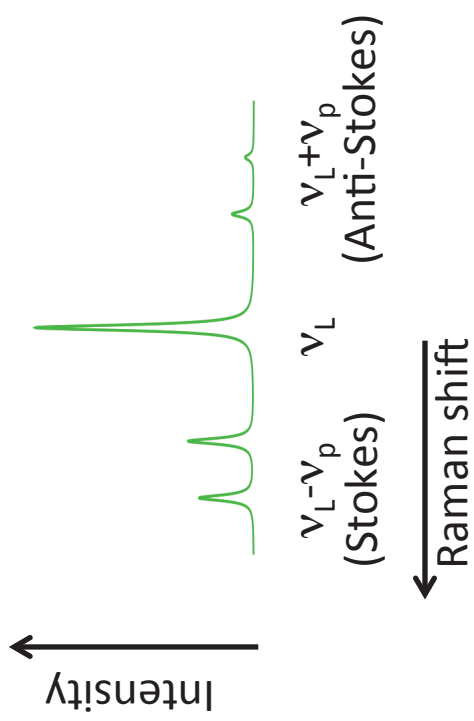
Here: introduction to the Double Resonance



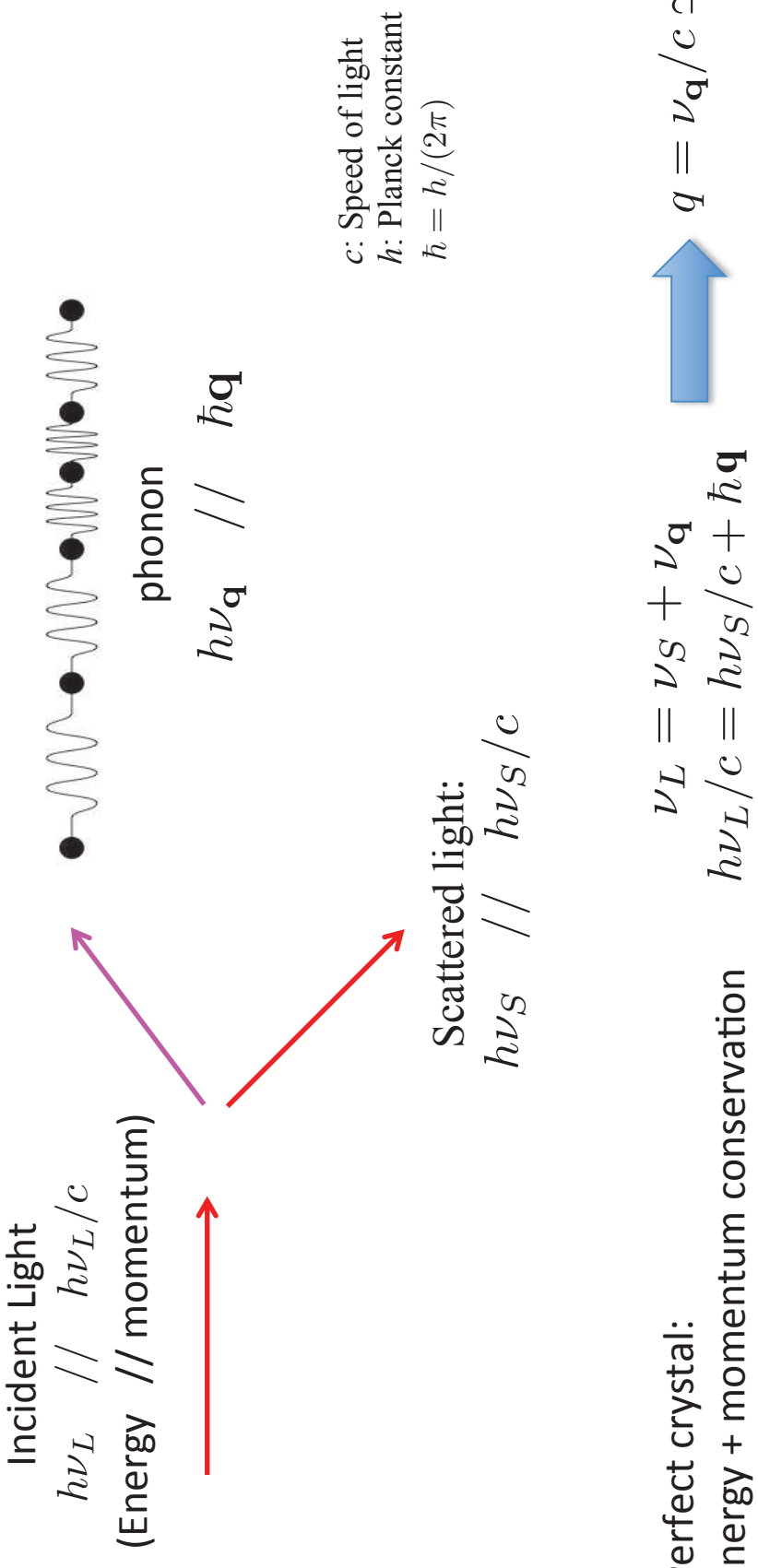
# Raman scattering



Frequency analyzer:



# Vibrational Raman



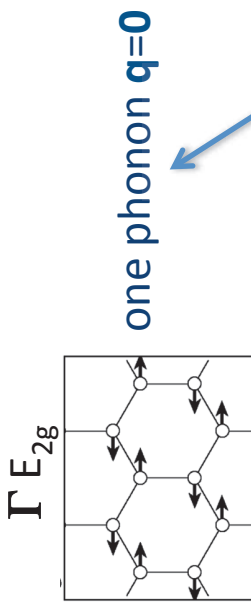
Most intense processes: one-phonon excitation  $\mathbf{q}=0$

Other possible processes:

Two-phonon excitation  $-\mathbf{q}, \mathbf{q} (\mathbf{q}\neq 0)$

Defect-activated one-phonon ( $\mathbf{q}\neq 0$ )

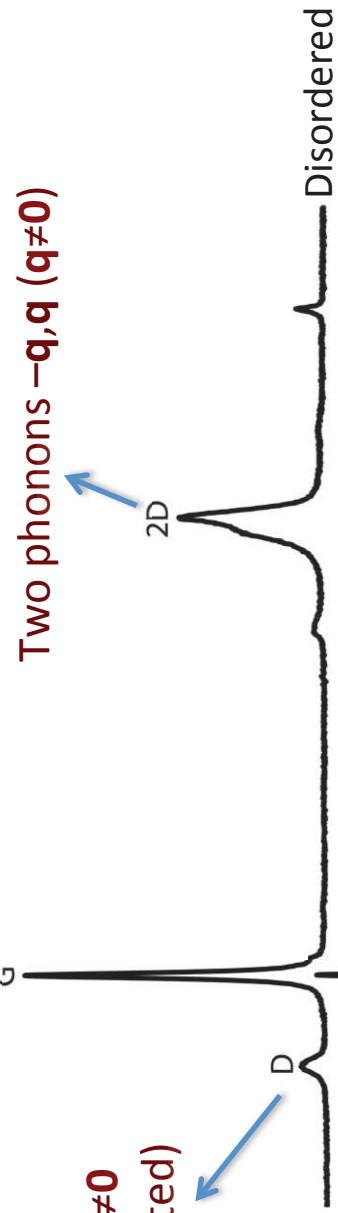
# Graphite Raman spectra



$\kappa A'_1$

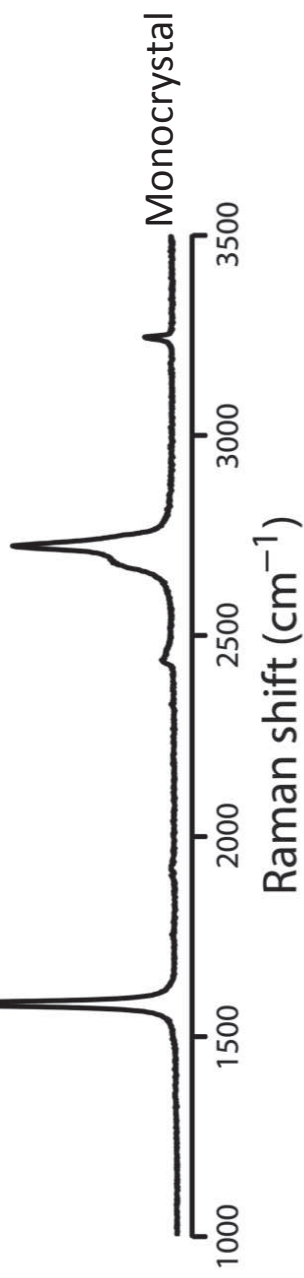
Two phonons  $-q, q$  ( $q \neq 0$ )

one phonon  $q \neq 0$   
(defect-activated)



G: « First-order » Raman

D/2D: Double resonance



# Why are the D/2D peaks so unique?

Anomalously high intensity  
Narrow peak, with well defined shape  
Frequency depends on the laser energy

Double resonance  
(Thomsen & Reich PRL 2000)

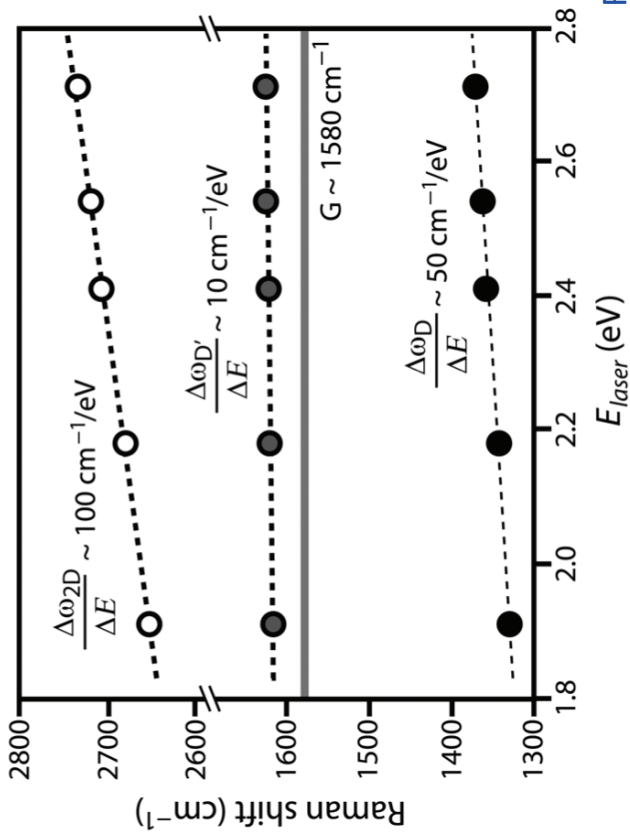
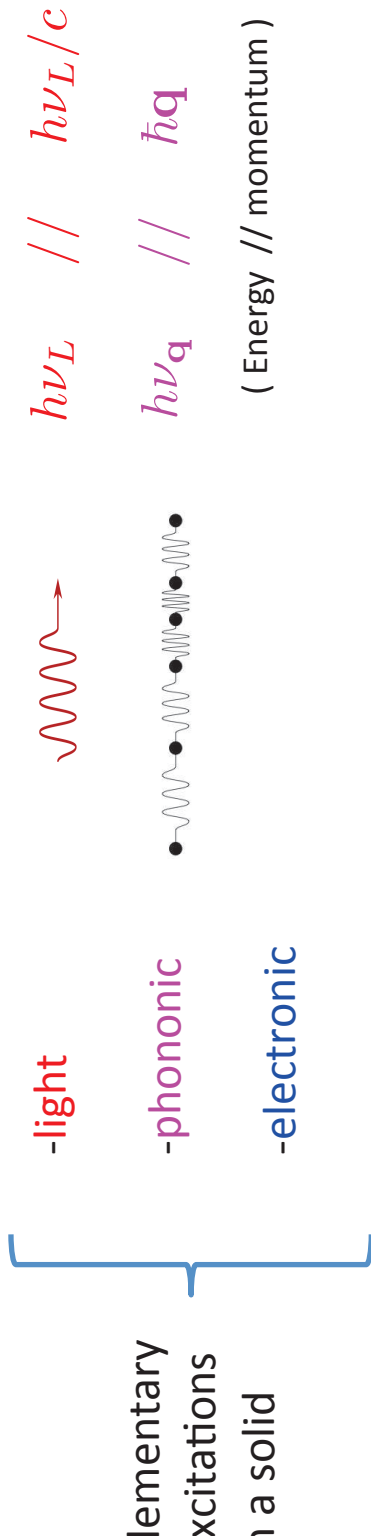


Fig. from Pimenta et al. PCCP (2007)

# Quantum mechanics: basic concepts

$|a\rangle$  : state of the system  
 $\epsilon_a$  : energy

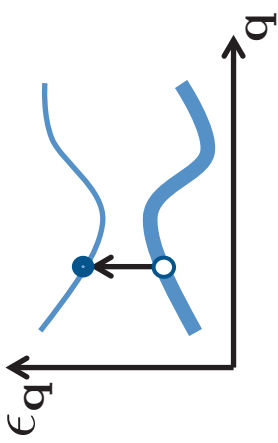
Ground state  $\rightarrow$  excitations



What is an electronic excitation?

$\epsilon_q$ : Band structure (the energies an electron is allowed to have)  
Ground state: lowest bands are occupied  
highest bands are empty

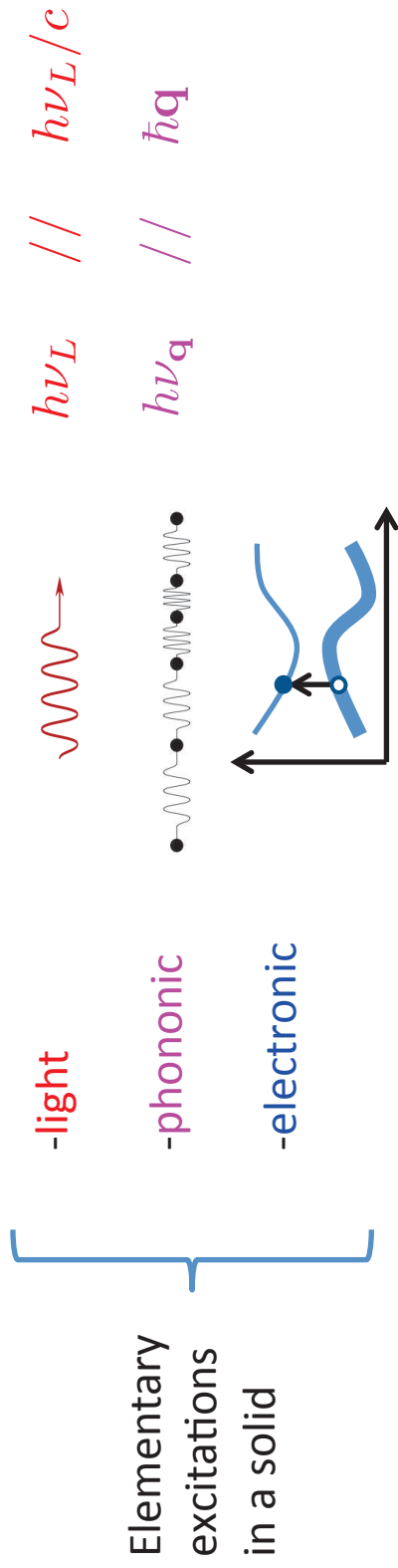
Excitation: creation of an electron/hole pair  
Vertical transition  $\rightarrow$  zero momentum



# Quantum mechanics: basic concepts

$|a\rangle$  : state of the system  
 $\epsilon_a$  : energy

Ground state  $\rightarrow$  excitations



$$|a\rangle = |\nu_L\rangle \otimes |\rho h\rangle \otimes |el\rangle$$

$$\text{Raman: } |i\rangle = |\nu_L\rangle \otimes |G\rangle \otimes |G\rangle \rightarrow |f\rangle = |\nu_S\rangle \otimes |\nu_p\rangle \otimes |G\rangle$$

# Perturbation theory (1st order)

$$V \quad \text{Interaction potential} \rightarrow P_{if} \quad (\text{Transition probability})$$

(e.g.: electron/light;  
electron/phonon;  
electron/defects)

Fermi Golden rule

(Basic assumption:  
 $V$  is small)

$$P_{if} = \frac{2\pi}{\hbar} |\langle i | V | f \rangle|^2 \delta(\epsilon_i - \epsilon_f)$$

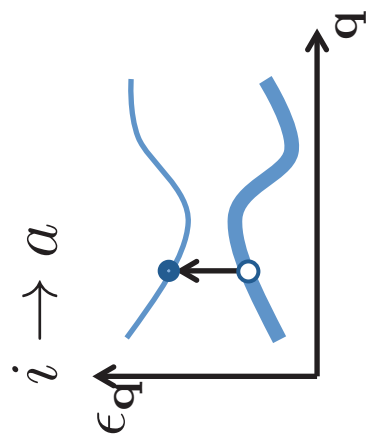
$\langle f | V | i \rangle$  Complex number which quantifies the interaction between  $i$  and  $f$   
(linear in  $V \rightarrow 1^{\text{st}} \text{ order}$ )

$$\delta(\epsilon) = 0 \quad \text{for } \epsilon \neq 0 \quad \Rightarrow \quad \epsilon_i = \epsilon_f \quad (\text{conservation of energy})$$

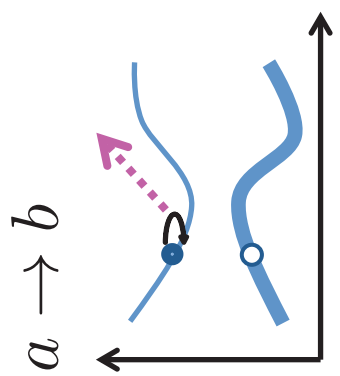
# Perturbation theory (3rd order)

$$P_{if} = \frac{2\pi}{\hbar} \left| \sum_{a,b} \frac{\langle i | V a \rangle \langle a | V b \rangle \langle b | V f \rangle}{(\epsilon_i - \epsilon_a - i\gamma)(\epsilon_i - \epsilon_b - i\gamma)} \right|^2 \delta(\epsilon_i - \epsilon_f)$$

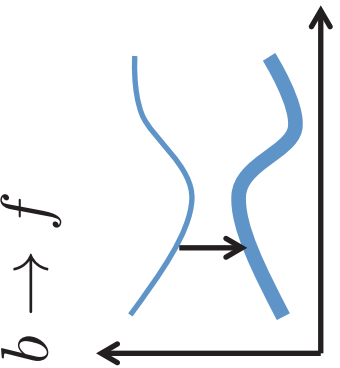
$\sum_a$ :Sum on all the possible excitations  
 $\gamma$ :Small real number  
 Raman scattering (one  $\mathbf{q}=0$  phonon)  
 3 consecutive « virtual transitions »:



Light absorption  
(electron/hole creation)



Electron/phonon scattering  
(phonon excitation)



Light emission  
(electron/hole recombination)

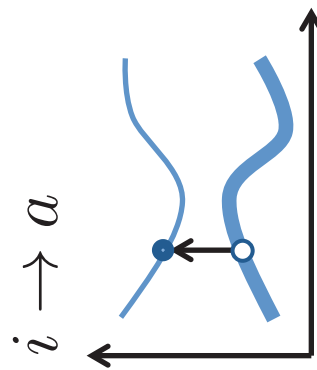
WARNING: In literature this is called « first-order » Raman

# Perturbation theory (4th order)

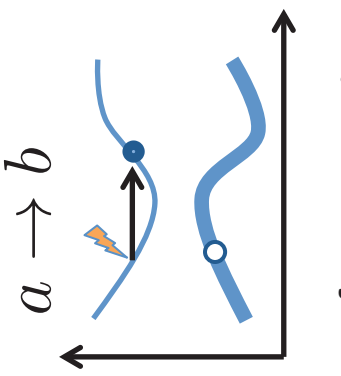
$$P_{if} = \frac{2\pi}{\hbar} \left| \sum_{a,b,c} \frac{\langle i | V a \rangle \langle a | V b \rangle \langle b | V c \rangle \langle c | V f \rangle}{(\epsilon_i - \epsilon_a - i\gamma)(\epsilon_i - \epsilon_b - i\gamma)(\epsilon_i - \epsilon_c - i\gamma)} \right|^2 \delta(\epsilon_i - \epsilon_f)$$

Raman scattering (one  $\mathbf{q} \neq 0$  phonon, defect activated)

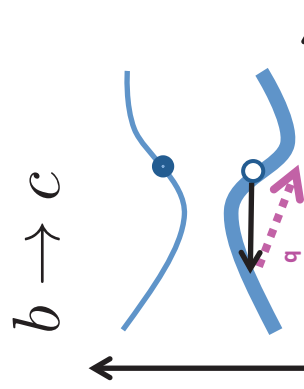
4 « virtual transitions »:



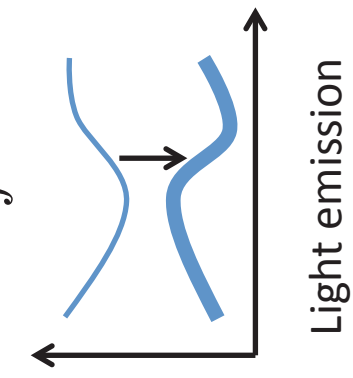
Light absorption



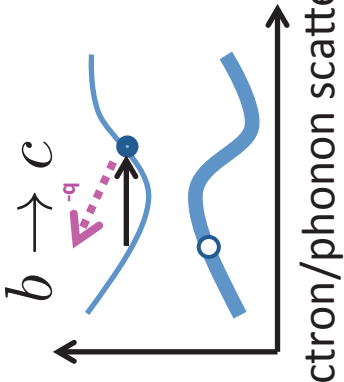
Defect scattering



Electr/phon scattering



Light emission



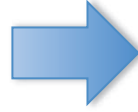
Two phonons - $\mathbf{q}, \mathbf{q}'$ :

Electron/phonon scattering

## Partial summary:

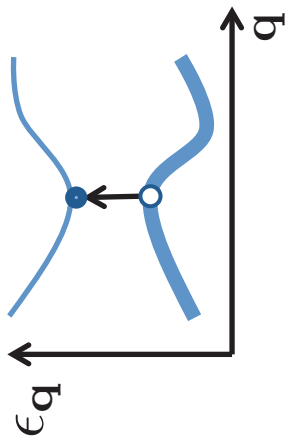
- Perturbation theory (standard textbook tool):
- 3rd order → excitation of one  $\mathbf{q}=0$  phonon
- 4th order → excitation of two-phonons
- excitation of one  $\mathbf{q}\neq\mathbf{0}$  phonon (defect-activated)

Why are the D/2D peaks so intense?  
Why are they small-width well defined peaks?  
Why do they disperse with the Laser energy?



Double resonance (Thomsen & Reich, PRL 2000)

# Resonant Raman



$E_g$  (electronic gap): minimum energy for electronic excitation

$E_g \neq 0 \rightarrow$  insulators/semiconductors

$E_g = 0 \rightarrow$  metals/semi-metals

$$\text{Raman: } P_{if} = \frac{2\pi}{\hbar} \left| \sum_{a,b} \frac{\langle iVa \rangle \langle aVb \rangle \langle bVf \rangle}{(\epsilon_i - \epsilon_a - i\gamma)(\epsilon_i - \epsilon_b - i\gamma)} \right|^2 \delta(\epsilon_i - \epsilon_f)$$

In the virtual transitions the energy is not necessarily conserved (e.g.  $\epsilon_i$  can be  $\neq \epsilon_a$ )

When  $\epsilon_i \approx \epsilon_a \rightarrow$  « resonance »

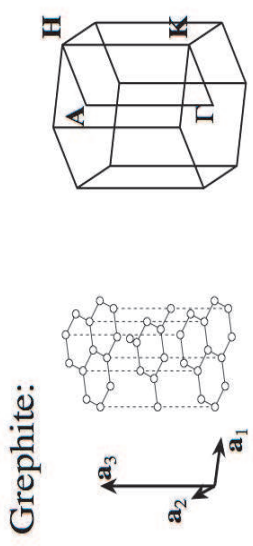
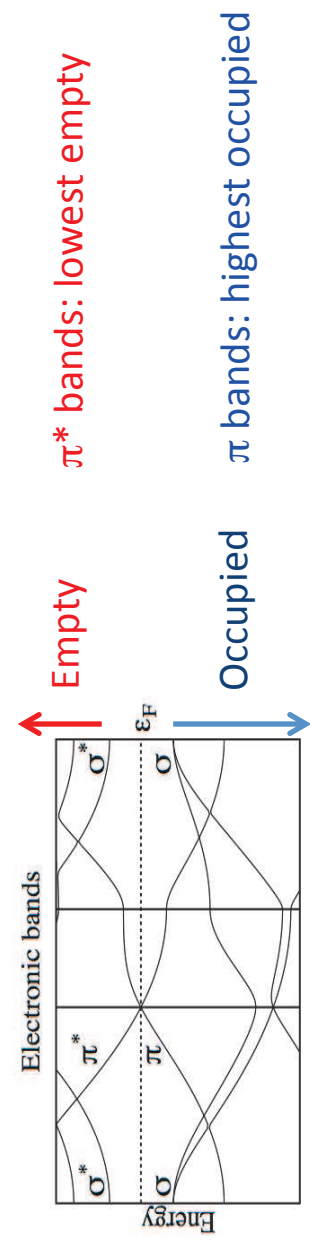
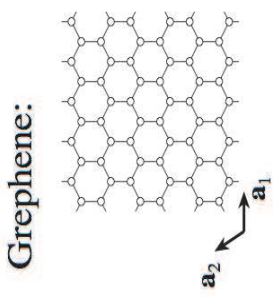
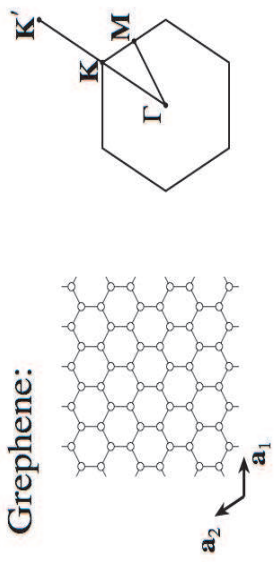
$E_g \gg h\nu_L$  : Non-Resonant Raman

$E_g = 0$  : Raman is always resonant

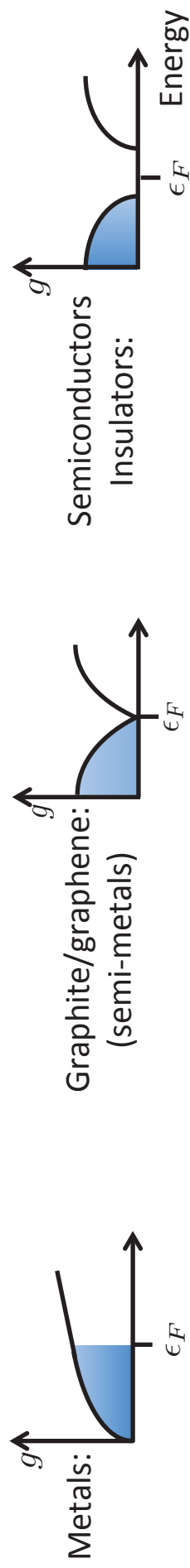
Graphite:  $E_g = 0 \rightarrow$  Raman is always resonant (the physics is more complex)

# Graphite: band structure

Graphene/graphite: very similar band structure and very similar Raman spectra.

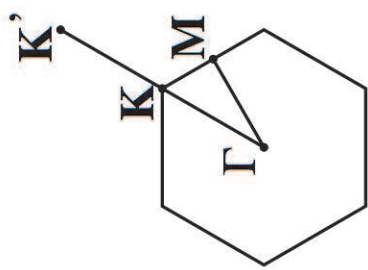
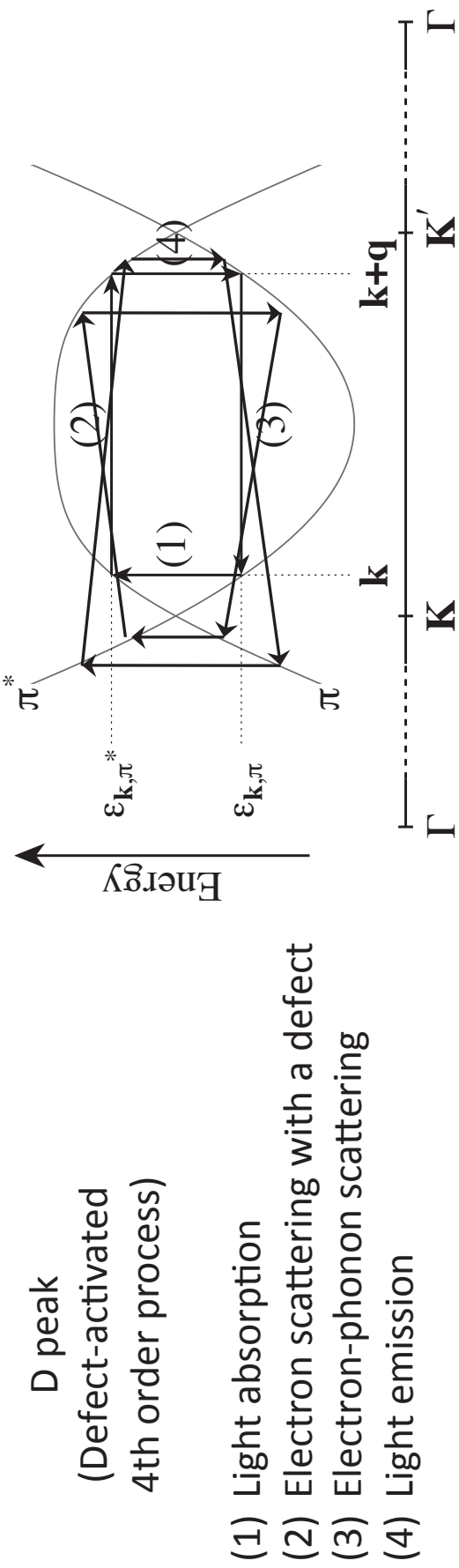


The « gap » is zero in  
only one point ( $\mathbf{K}$ ) of  
the Brillouin zone



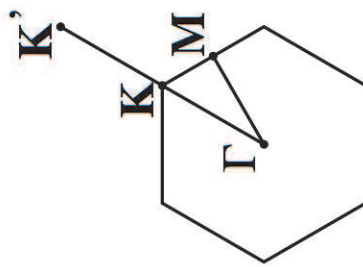
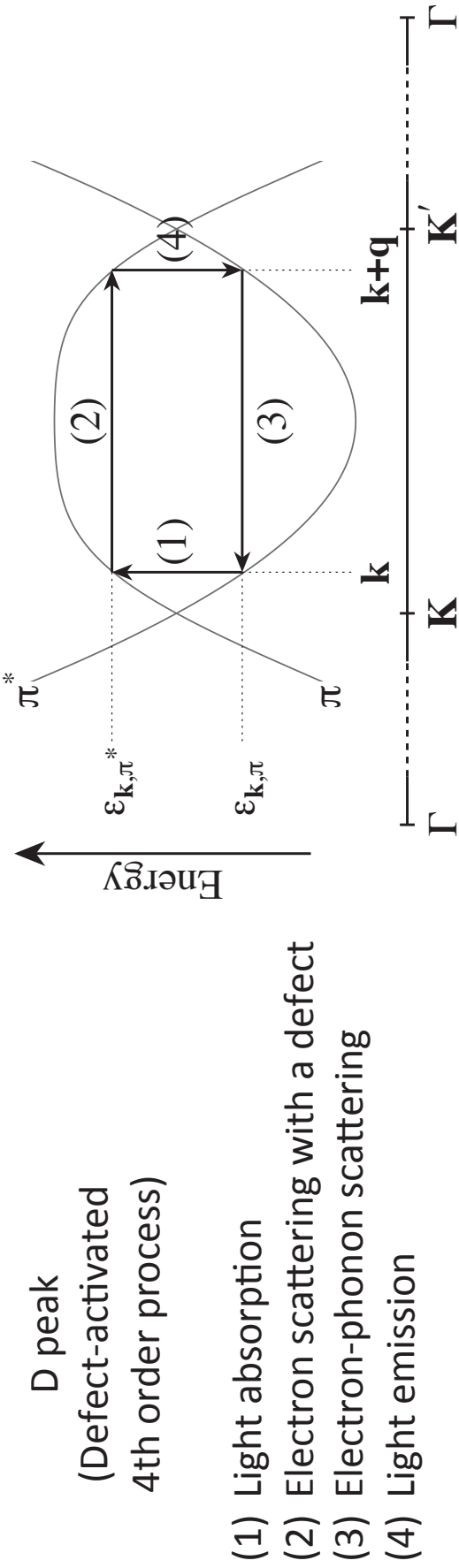
$g = \#$  of electronic states at a given energy  
 $\epsilon_F$  = Fermi level

# Double Resonance in graphite/graphene



In principle: all the possible processes have to be considered

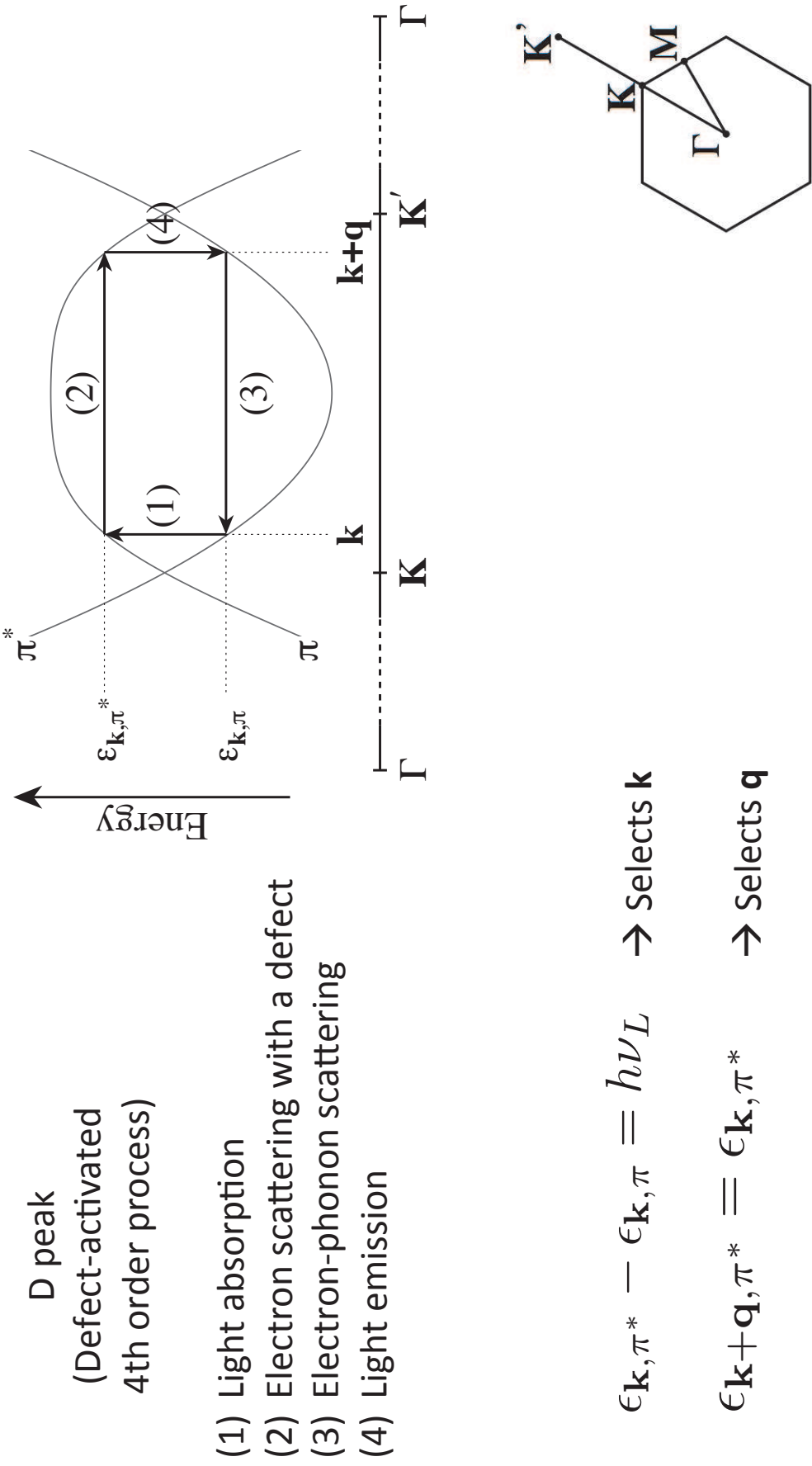
# Double Resonance in graphite/graphene



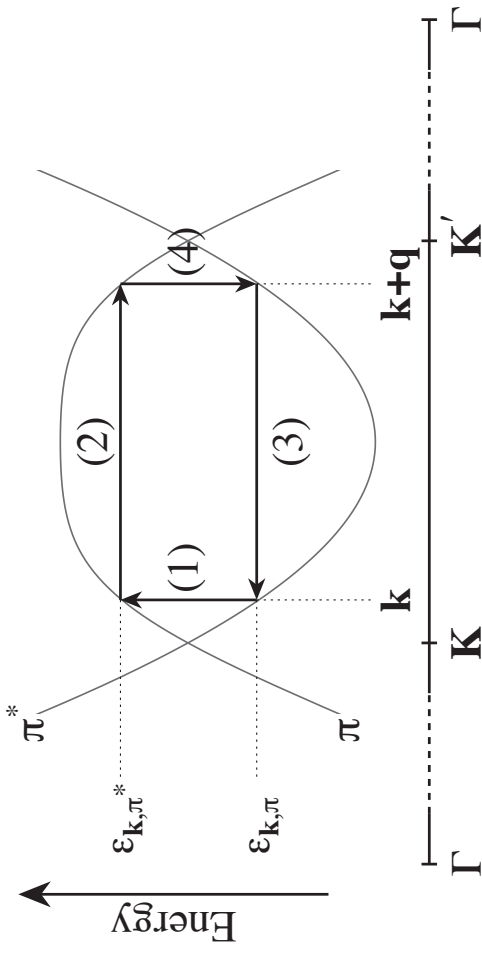
In general: all the possible processes have to be considered

Thomsen & Reich (2000): The important processes take place only for certain values of  $k$  and  $q$  (selected by the conservation of energy in the virtual transitions)

# Double Resonance in graphite/graphene



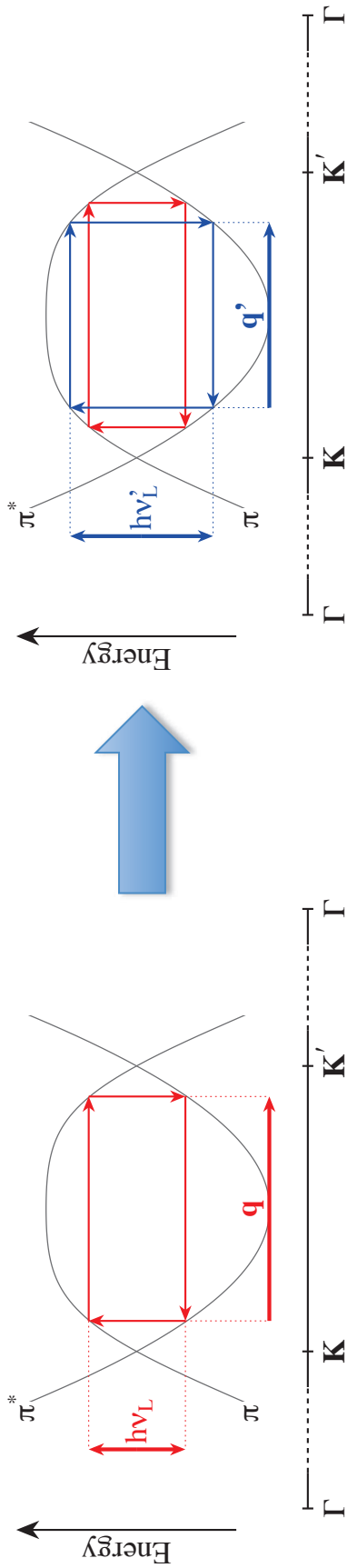
# Double Resonance in graphite/graphene



Double resonance explains:

- Anomalously high intensity of D/2D peaks
- They are well-defined small-width peaks (not broad bands)
- The actual origin of the defect does not play a role

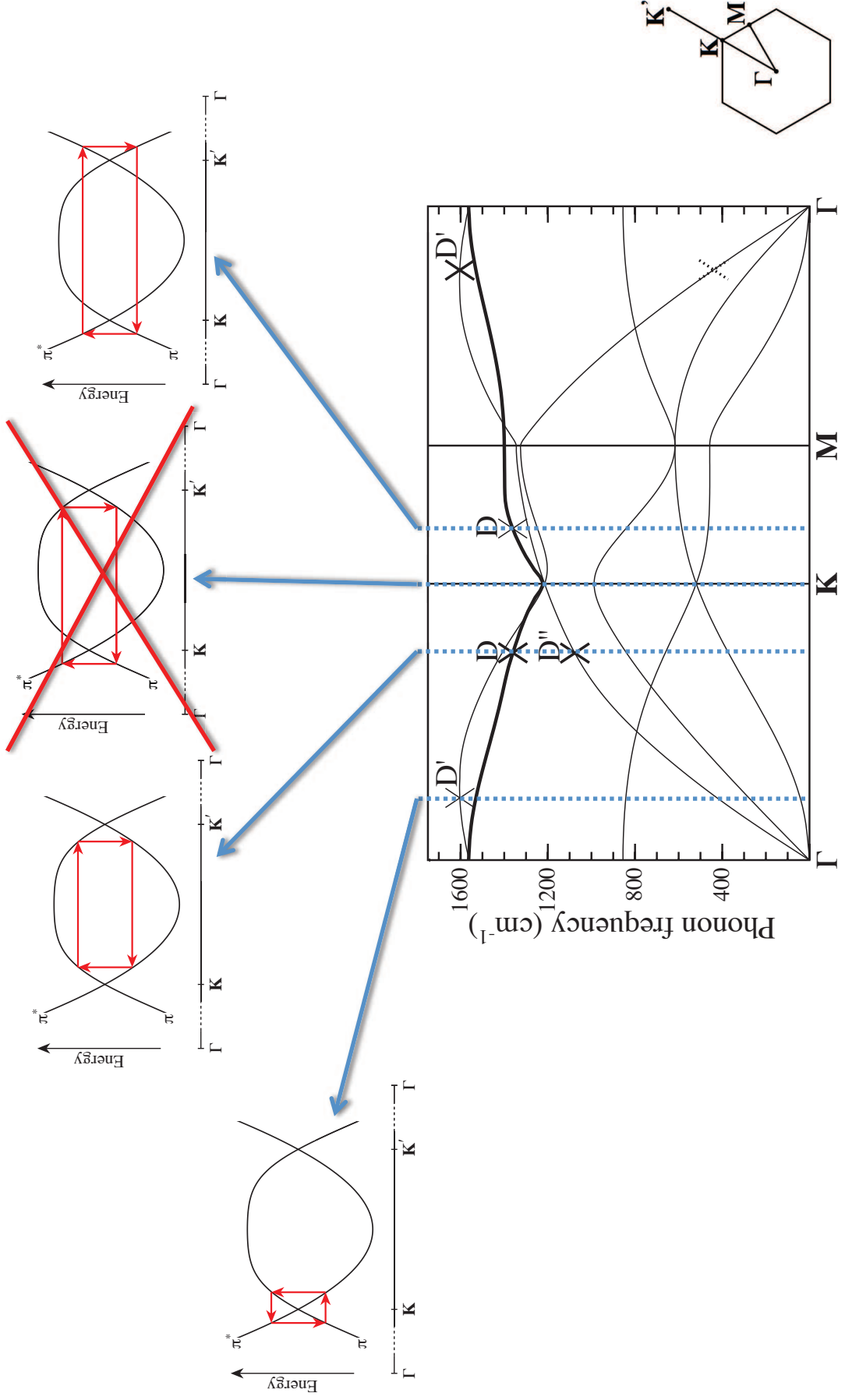
# Double Resonance in graphite/graphene



Double resonance explains:

- Anomalously high intensity of D/2D peaks
- They are well-defined small-width peaks (not broad bands)
- The actual origin of the defect does not play a role
- The peaks shift by changing the laser energy

# Attribution of the Raman peaks



# Attribution of the Raman peaks

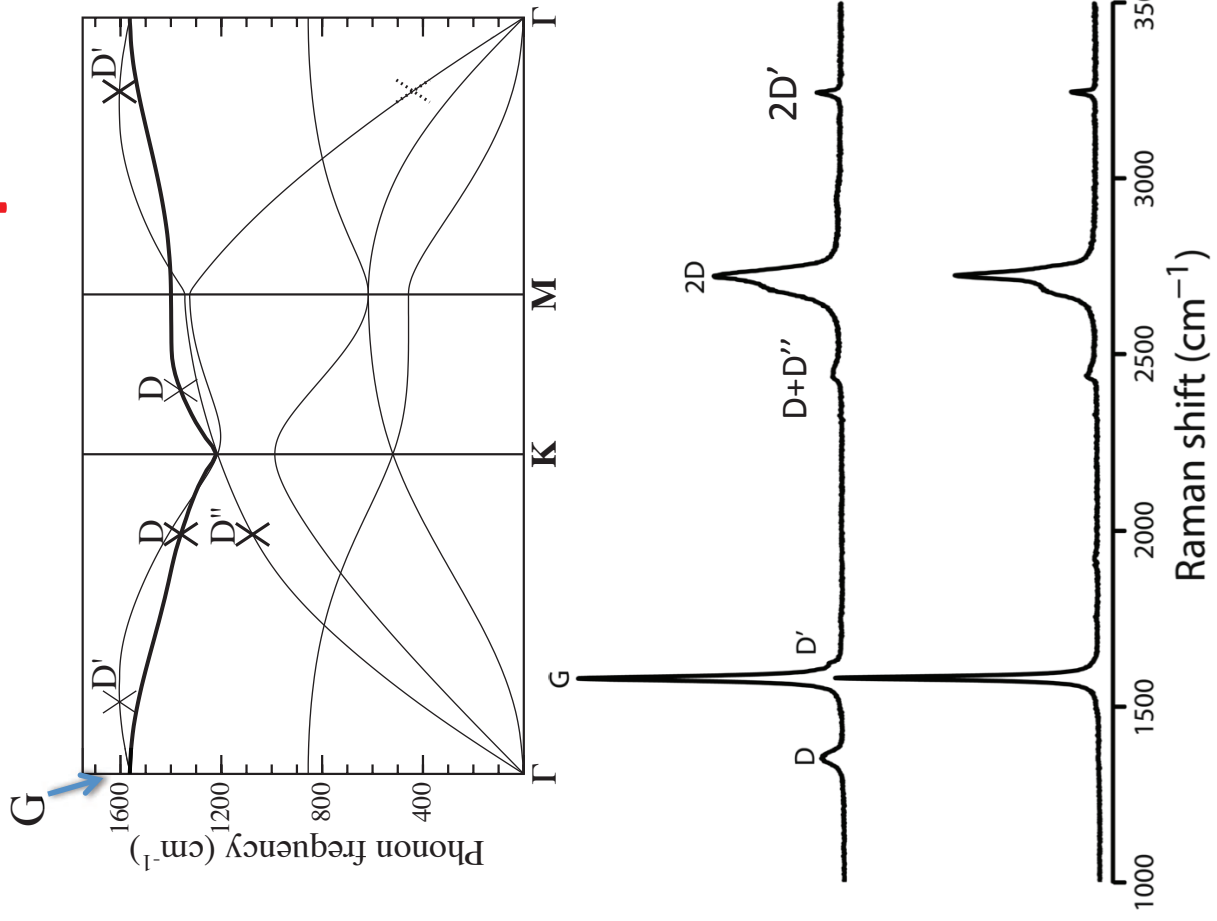
Lowest-order:  
 $G \rightarrow 1580 \text{ cm}^{-1}$

## Double resonant:

- 1) Defect-activated:  
 $D \rightarrow 1350 \text{ cm}^{-1}$   
 $D' \rightarrow 1620 \text{ cm}^{-1}$

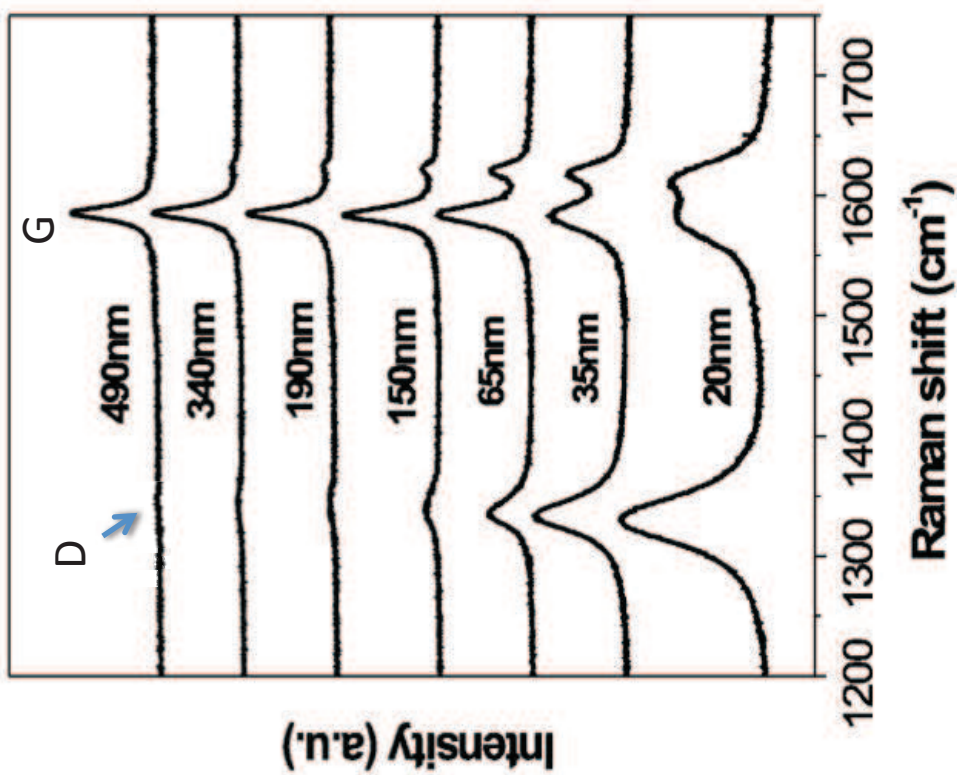
## 2) Two-phonon:

- $D+D'' \rightarrow 2450 \text{ cm}^{-1}$
- $2D \rightarrow 2700 \text{ cm}^{-1}$
- $2D' \rightarrow 3240 \text{ cm}^{-1}$



$$\lambda_L = 514 \text{ nm}$$

# Raman as a tool to measure disorder



Can we quantify the disorder through  
the D peak?

Tuinstra & Koenig relation (1970):

$$\frac{I_D}{I_G} \propto \frac{1}{L_a}$$

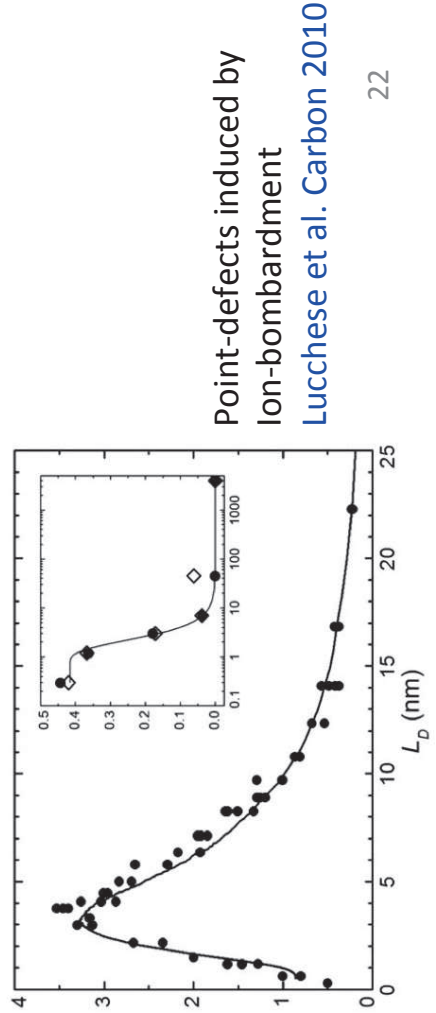
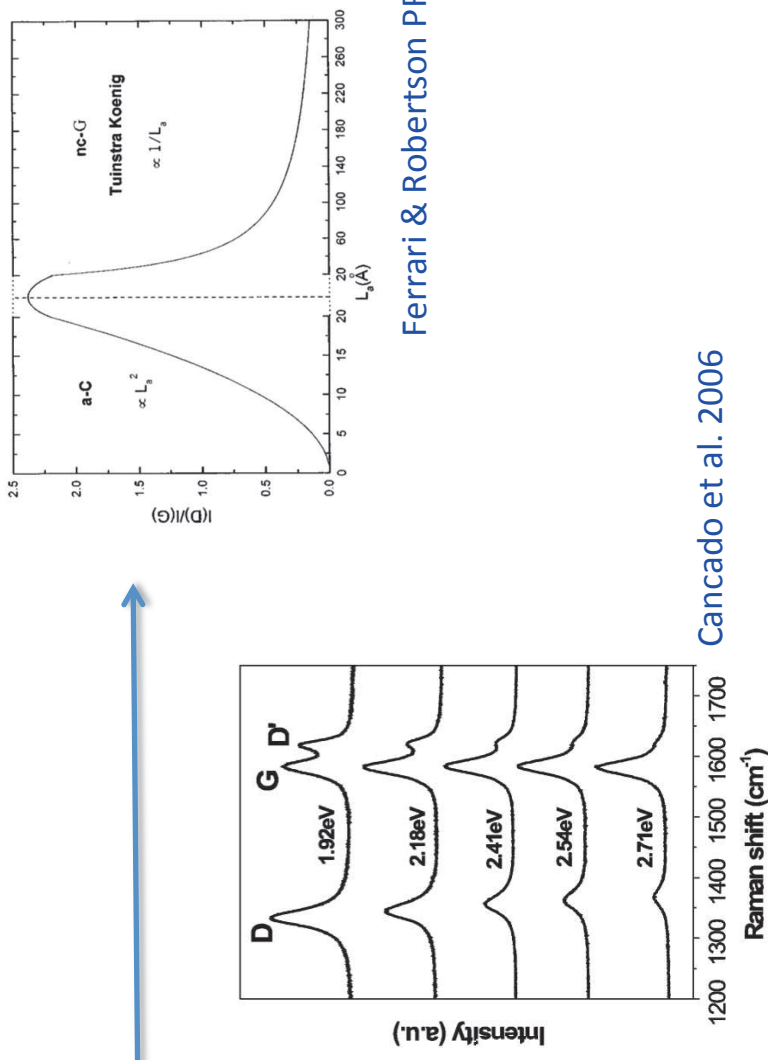
$L_a$  = crystallite size

Fig. from Pimenta et al PCCP 2007

# Validity limits of the TK relation

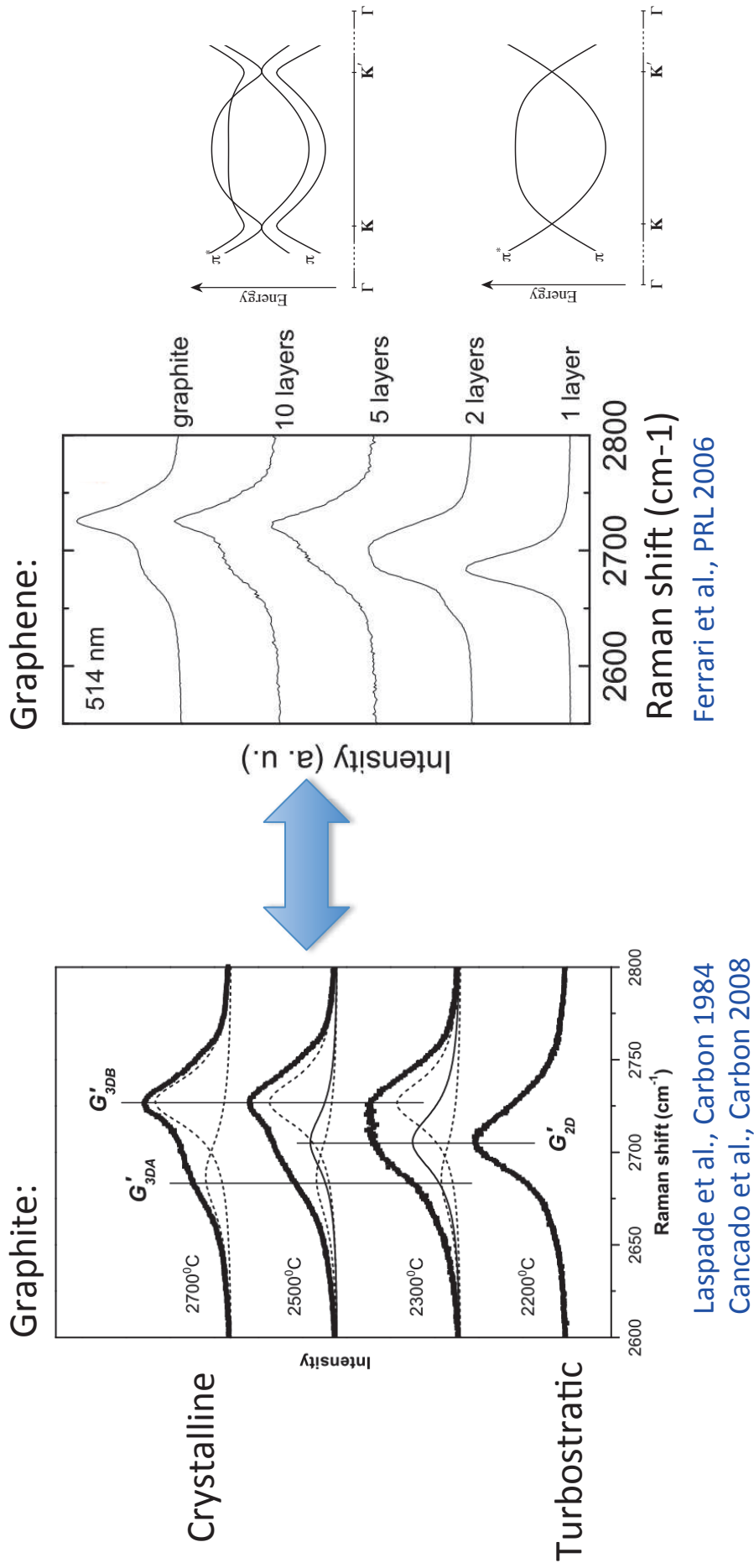
$I_D/I_G \propto 1/L_a$   
only for  
 $L_a > 2$  nm

$I_D/I_G$   
depends also on  $\nu_L$



The D peak can be activated by other sources of disorder!

# 2D shape and stacking order



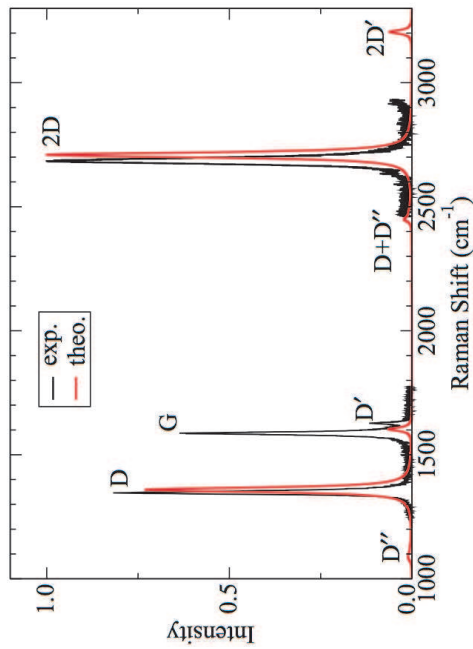
The 2D shape provides information on the stacking order

# Conclusions

This talk: introduction to the Double Resonant Raman  
in graphite (model sp<sub>2</sub> carbon system)

2000: Thomsen & Reich → explanation of the general characteristics of the spectra

Nowadays: quantitative approach to  
describe Raman spectra in controlled  
experimental situations



Venezuela et al. PRB 2011

Characterization of natural samples is still heavily based on phenomenological model